

Electronic Supplementary Information for

Enhanced crystal network and charge transfer of non-fused ring electron acceptor via interchain interaction enable efficient and stable organic solar cells

Shounuan Ye,^{‡a} Tianyi Chen,^{‡a} Jinyang Yu,^a Shanlu Wang,^a Shuixing Li,^{*b} Jingxi Wang,^a Yuang Fu,^c Yuxuan Zhu,^d Mengting Wang,^a Xinhui Lu,^c Zaifei Ma,^d Chang-Zhi Li,^a Minmin Shi^{*a} and Hongzheng Chen^{*ab}

^a MOE Key Laboratory of Macromolecular Synthesis and Functionalization, State Key Laboratory of Silicon and Advanced Semiconductor Materials, Department of Polymer Science and Engineering, Zhejiang University, Hangzhou 310027, P. R. China. E-mail: minminshi@zju.edu.cn; hzchen@zju.edu.cn

^b Zhejiang University-Hangzhou Global Scientific and Technological Innovation Center, Hangzhou 311200, P. R. China. E-mail: lishuixing89@zju.edu.cn

^c Department of Physics, The Chinese University of Hong Kong, Hong Kong 999077, P. R. China

^d State Key Laboratory for Modification of Chemical Fibers and Polymer Materials, Center for Advanced Low-dimension Materials, College of Materials Science and Engineering, Donghua University, Shanghai 201620, P. R. China

[‡] S. Ye. and T. Chen. contributed equally to this work.

Characterization

NMR & MS

¹H-NMR spectra were obtained on a Bruker Advance III 400 (400 MHz) NMR spectroscope. Matrix-assisted laser desorption/ionization time-of-flight (MALDI-TOF) mass spectrum tests were carried out on a Bruker Ultraflextreme MALDI-TOF/TOF mass spectrometry.

Thermal Analysis

Thermogravimetric analysis (TGA) was done on a WCT-2 thermal balance under N₂ atmosphere at a heating rate of 10 °C/min. Differential scanning calorimetry (DSC) was recorded on a Pekin-Elmer Pyris 1 differential scanning calorimeter.

Density functional theory (DFT)

Density functional theory calculations were conducted at the B3LYP/6-31G(d) level to obtain the optimized molecular geometries and frontier molecular orbitals of the acceptors. The outward *n*-octyl of the three acceptors were replaced with methyl groups for simplified calculations.

Absorption & Energy Levels

UV-vis absorption spectra were recorded on a HITACHI U-4100 spectrophotometer. Cyclic voltammetry (CV) measurements were carried out on a CHI600A electrochemical workstation with Pt plate as the working electrode, Pt wire as the counter electrode, and standard calomel electrode (SCE) as the reference electrode in anhydrous acetonitrile solution containing 0.1 mol/L tetrabutylammonium hexafluorophosphate (Bu₄NPF₆) as the supporting electrolyte. All potentials were corrected against ferrocene/ferrocenium (Fc/Fc⁺) whose absolute energy level is 4.8 eV below vacuum. The equation of $E_{\text{LUMO/HOMO}} = -e(E_{\text{red/ox}} + 4.41)$ (eV) was used to calculate the LUMO and HOMO levels (the redox potential of Fc/Fc⁺ is found to be 0.39 V).

Single Crystal

The crystals of acceptors were grown by solvent diffusion. Acceptor (~20 mg) was dissolved in ~2 mL CHCl₃ and placed in a culture tube (7 × 200 mm) with layered methanol upon it. The tube was then sealed tightly and left undisturbed for 14 days.

X-ray crystallographic data were collected at Bruker Single Crystal X-RAY Diffraction D8 Venture. The structure was solved by the intrinsic phasing method (SHELXT) and refined by the least-squares method (SHELXL) integrated in Olex2.

Device Fabrication

Organic photovoltaics were fabricated on glass substrates commercially pre-coated with a layer of indium tin oxide (ITO) with the conventional structure of ITO/PEDOT:PSS/Active layer/PDINN/Ag. Before fabrication, the substrates were

cleaned using detergent, deionized water, acetone, and isopropanol consecutively for 10 min in each step. And then the ITO substrates were treated in the ultraviolet cleaner (UC100-SE, LEBO Science) for 10 min before being spin-coated at 4500 rpm with a layer of 10 nm thickness PEDOT:PSS (Clevios™ 4083). After baking the PEDOT:PSS layer in air at 150 °C for 10 min, the substrates were transferred to the N₂ glovebox. The D:A ratio is 1:1.2 (w/w) for all blends, and the total concentration is 10 mg mL⁻¹. Heat and stir at 60 °C for 1 hour before spin coating. Then an annealing at 90 °C for 5 min was performed. A thin layer of PDINN was spin-coated from 1.5 mg mL⁻¹ methanol solution on the top of the active layer. Finally, the Ag (100 nm) electrode was deposited by thermal evaporation to complete the device with an active area of 6 mm², and the testing aperture area is 4.572 mm².

***J-V* and EQE Measurement**

The *J-V* measurement was performed via the solar simulator (SS-X50, Enlitech) and AM 1.5G spectra, calibrating the intensity of the certified standard silicon solar cell (KG2) at 100 mW cm⁻². The external quantum efficiency (EQE) data were obtained using the solar-cell spectral-response measurement system (RE-R, Enlitech).

Space Charge Limited Current (SCLC) Measurement

The charge carrier mobilities of the blended films were measured using the space-charge-limited current (SCLC) method. Hole-only devices were fabricated in a structure of ITO/PEDOT:PSS/Active layer/MoO₃/Ag, and electron-only devices were fabricated in a structure of ITO/ZnO/Active layer/PDINN/Ag. The device characteristics were extracted by modeling the dark current under forward bias using the SCLC expression described by the Mott-Gurney law¹:

$$J = \frac{9}{8} \varepsilon_r \varepsilon_0 \mu \frac{V^2}{L^3}$$

where $\varepsilon_r \approx 3$ is the average dielectric constant of the blended film, ε_0 is the permittivity of the free space, μ is the carrier mobility, L is the thickness of the film (~100 nm), and V is the applied voltage.

Electroluminescence External Quantum Efficiency (EQE_{EL})

A digital source meter (Keithley 2400) and a picoammeter (Keithley 6482) were used for the EQE_{EL} measurements. The former was applied to inject electric current into the solar cells to emit the photons, which will be collected using a Si diode and form electric current that can be measured by the latter.

Electroluminescence (EL) Measurement

A source meter (Keithley 2400) was employed to create the injected electric current leading to the luminescence of the solar cells. After going through an optical fiber (BFL200LS02, Thorlab), the emitted light emerged from the solar cells was collected by a fluorescence spectrometer (KYMERA-3281-B2, Andor Technology) including two sets of diffraction gratings for the wavelength range of 600~1100 nm and

900~1400 nm, and was measured by a Si EMCCD camera (DU970PBVF, Andor Technology) and an InGaAs camera (DU491A-1.7, Andor Technology), respectively.

The EL spectra were corrected for the optical losses in the fibers, the spectrometer and the cameras, using a calibrated halogen lamp (HL-3P-CAL, Ocean Optics Germany GmbH).

Photoluminescence (PL) Measurement

A Supercontinuous White Laser (SuperK EXU-6, NKT photonics) and narrowband filters (LLTF Contrast SR-VIS-HP8, LLTF Contrast SR-SWIR-HP8, NKT photonics) were used to acquire the tunable excitation wavelength. After excited by the laser, the measurement processes of the emission spectra were the same as electroluminescence spectra.

The PL spectra were corrected for the optical losses as same as EL spectra. In addition, the PL spectra were also corrected for excluding the difference of the absorption ability caused by thickness between different organic layers when characterize the photoluminescence quenching efficiency.

Transient Absorption Spectroscopy (TAS) Measurement

For femtosecond transient absorption spectroscopy, the fundamental output from Yb:KGW laser (1030 nm, 220 fs Gaussian fit, 100 kHz, Light Conversion Ltd) was separated to two light beams. One was introduced to NOPA (ORPHEUS-N, Light Conversion Ltd) to produce a certain wavelength for pump beam (here we use 750 nm, $10 \mu\text{J}/\text{cm}^2$), the other was focused onto a YAG plate to generate white light continuum as probe beam. The pump and probe overlapped on the sample at a small angle less than 10° . The transmitted probe light from sample was collected by a linear CCD array. Then we obtained transient differential transmission signals by equation shown below:

$$\frac{\Delta T}{T} = \frac{T_{\text{pump-on}} - T_{\text{pump-off}}}{T_{\text{pump-off}}}$$

We processed the analysis of hole transfer kinetics by biexponential fitting based on the following formula:

$$i = A_1 e^{-t/\tau_1} + A_2 e^{-t/\tau_2}$$

GIWAXS Measurement

GIWAXS measurements were performed in a Xeuss 3.0 SAXS/WAXS system with a wavelength of $\lambda = 1.54189 \text{ \AA}$ at Vacuum Interconnected Nanotech Workstation (Nano-X).

Contact Angle

Contact angle test was conducted on a LAUDA Scientific LSA series video optical contact angle tension measuring instrument.

AFM Measurement

The morphologies of blended films were characterized by a VeecoMultiMode atomic force microscopy (AFM) in the tapping mode.

FT-IR Measurement

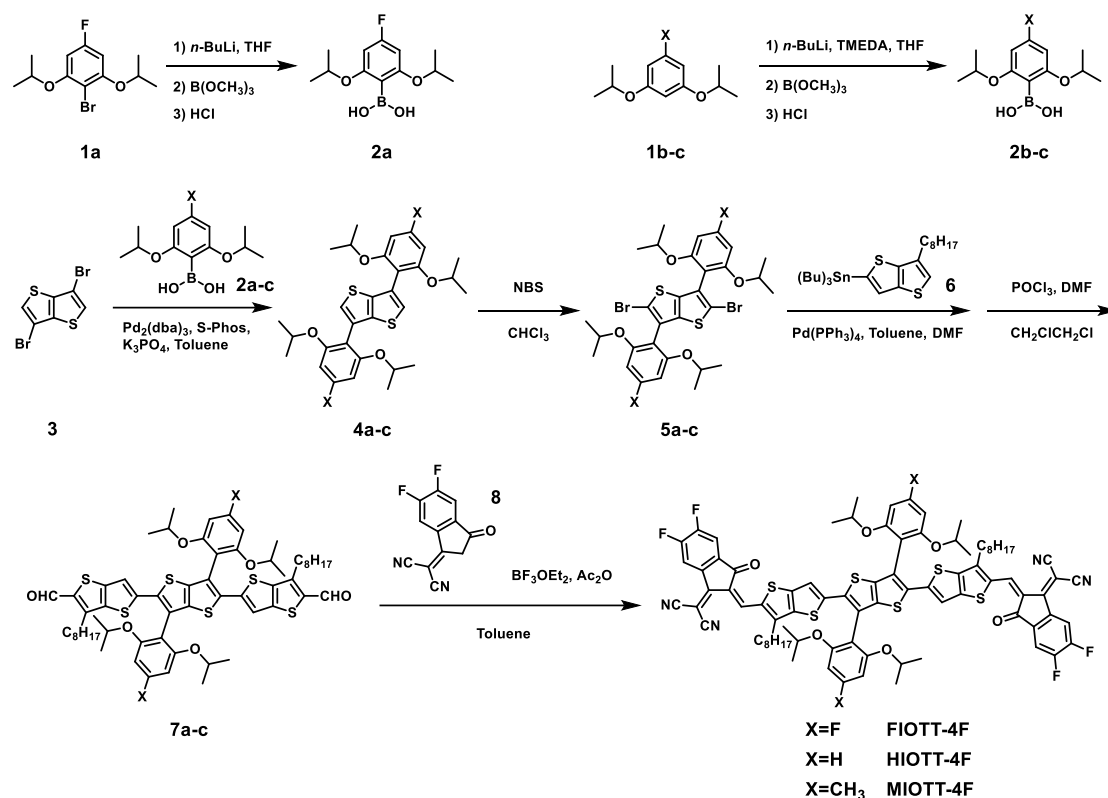
Fourier transform infrared spectroscopy (FT-IR) measurements were conducted on a Nicolet 6700 FTIR-ATR (Thermo Fisher scientific LLC).

SNOM Measurement

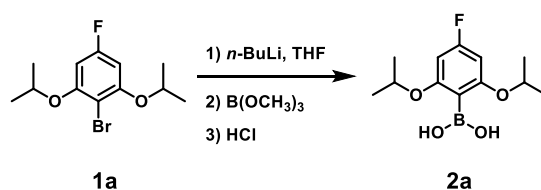
Scanning near-field optical microscopy (SNOM) images were obtained on nanoIR2-fs (Anasys Instruments) in the contact mode.

Materials

Compound 1a was synthesized according to the literature method^{2,3}. Compound 6 was purchased from Zhengzhou huijuchem Co., Ltd. Compound 8 was purchased from Derthon Optoelectronics Materials Science Technology Co., Ltd. D18 was purchased from Solarmer Materials Inc. PDINN was purchased from Organtec Ltd. PEDOT:PSS (P Al 4083) was purchased from Heraeus CleviosTM. Other reagents and solvents were commercially available and used without further purification.



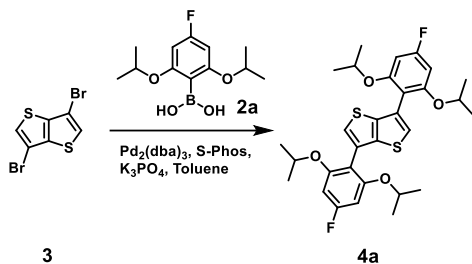
Scheme S1 Synthetic routes of FIOTT-4F, HIOTT-4F and MIOTT-4F.



Compound 2a:

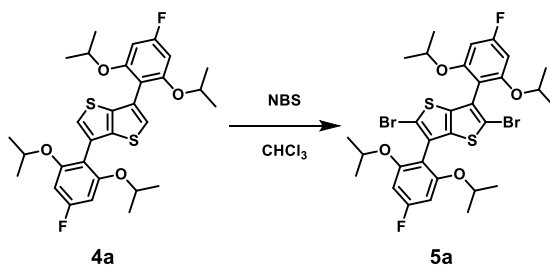
To a solution of Compound 1a (6000 mg, 20.60 mmol) in 80 mL dry THF, *n*-BuLi (11.2 mL, 2.4 M, 26.80 mmol) was added dropwise under the protection of argon at -78 °C. After the mixture was stirred at -78 °C for 1 h, B(OCH₃)₃ (4282 mg, 41.22 mmol) was added in one portion. Then the mixture was stirred overnight and allowed to warm up to room temperature gradually. After quenched with 100 mL 1 M HCl, the mixture was stirred for 3 h and then extracted with dichloromethane. The combined organic phase was evaporated under vacuum. The obtained product was used directly in the next

reaction without further purification, yielding a colorless solid (4484 mg, 85%). ^1H NMR (400 MHz, Chloroform-*d*) δ 7.28 (s, 2H), 6.31 (d, $J = 10.9$ Hz, 2H), 4.62 (hept, $J = 6.1$ Hz, 2H), 1.41 (d, $J = 6.1$ Hz, 12H).



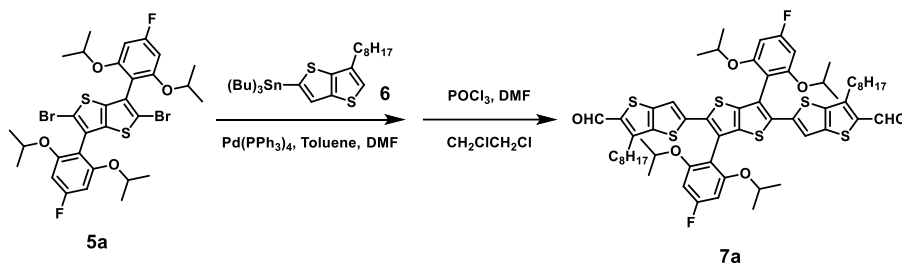
Compound 4a:

Compound 3 (665 mg, 2.23 mmol), Compound 2a (2280 mg, 8.90 mmol), and potassium phosphate tribasic (K_3PO_4) (3314 mg, 15.61 mmol) were added in toluene (30 mL). The mixture was frozen by liquid nitrogen, followed by three times of successive vacuum and argon fill cycles. Then, $\text{Pd}_2(\text{dba})_3$ (119 mg, 0.13 mmol) and 2-dicyclohexylphosphino-2',6'-dimethoxybiphenyl (S-Phos) (107 mg, 0.26 mmol) were added and another three times of successive vacuum and argon fill cycles were performed. The mixture was refluxed at 110 $^\circ\text{C}$ for 48 h. After pouring into the water, the mixture was extracted with dichloromethane. The combined organic phase was evaporated under vacuum. The obtained crude product was purified through column chromatography with the mixture of petroleum ether and dichloromethane (3:2, v/v) to afford Compound 4a as a white solid (1013 mg, 81%). ^1H NMR (400 MHz, Chloroform-*d*) δ 7.27 (s, 2H), 6.39 (d, $J = 10.7$ Hz, 4H), 4.31 (hept, $J = 6.1$ Hz, 4H), 1.18 (d, $J = 6.0$ Hz, 24H).



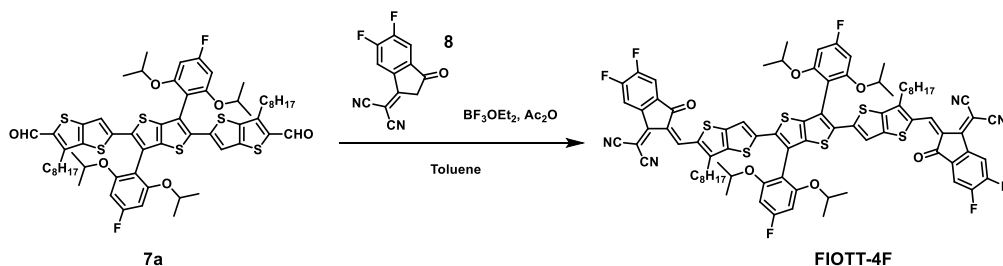
Compound 5a:

To a solution of compound 4a (935 mg, 1.67 mmol) in 20 mL CHCl_3 , N-succinbromimide (NBS) (608 mg, 3.42 mmol) was added and stirred dark at 0 $^\circ\text{C}$ for about 10 min (monitored by TLC). After the solvent was evaporated, methanol was added and filtered. The product was dried in vacuum to yield a white solid (1140 mg, 95%). ^1H NMR (400 MHz, Chloroform-*d*) δ 6.36 (d, $J = 10.8$ Hz, 4H), 4.33 (hept, $J = 5.9$ Hz, 4H), 1.22 – 1.15 (m, 24H).



Compound 7a:

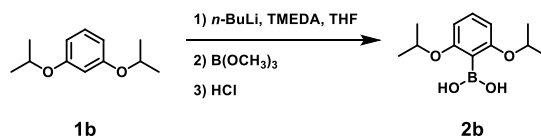
Compound 5a (600 mg, 0.84 mmol) and Compound 6 (1130 mg, 2.09 mmol) were dissolved in toluene (20 mL) and DMF (5 mL). The mixture was frozen by liquid nitrogen, followed by three times of successive vacuum and argon fill cycles. Then, Pd(PPh₃)₄ (58 mg, 0.05 mmol) was added and another three times of successive vacuum and argon fill cycles were performed. The mixture was refluxed at 120 °C overnight. After cooling to room temperature, the mixture was diluted with petroleum ether and quickly passed through a silica gel column with dichloromethane as the eluent. After the solvent was removed by rotary evaporation, the mixture was dissolved with 1,2-dichloroethane and injected into the Vilsmeier-Haack reagent (freshly prepared by 0.5 mL POCl₃ and 1 mL DMF at 0 °C under argon). The mixture was heated to 70 °C and kept for about 2 h (monitored by TLC). After cooling to room temperature, the mixture was poured slowly into a saturated sodium bicarbonate solution and stirred for another 4 h. The crude product was extracted with dichloromethane and dried over anhydrous Na₂SO₄. After removing the solvent, silica gel column chromatography was used to purify the product with the mixture of petroleum ether and dichloromethane (1:1~1:4, v/v) as the eluent, yielding an orange solid (657 mg, 70% in total). ¹H NMR (400 MHz, Chloroform-*d*) δ 10.01 (s, 2H), 7.12 (s, 2H), 6.39 (d, *J* = 10.7 Hz, 4H), 4.43 – 4.25 (m, 4H), 3.06 – 2.94 (m, 4H), 1.77 – 1.65 (m, 4H), 1.34 – 1.21 (m, 20H), 1.16 (d, *J* = 5.6 Hz, 12H), 0.99 (d, *J* = 5.6 Hz, 12H), 0.88 (t, *J* = 6.1 Hz, 6H).



FIOTT-4F:

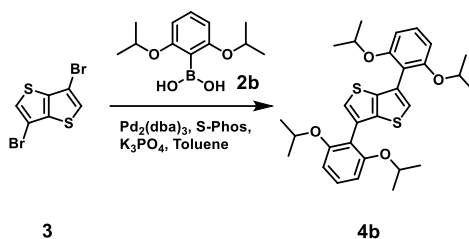
FIOTT-4F was prepared by the method from the literature report⁴. Compound 7a (210 mg, 0.19 mmol) and Compound 8 (95 mg, 0.41 mmol) were dissolved in toluene (20 mL). Then, BF₃OEt₂ (336 mg, 2.35 mmol) and Ac₂O (0.2 mL) was injected and the mixture was stirring at room temperature for 1 h. Once the reaction was completed, the mixture was poured into methanol and the filtered solid was purified by silica gel column chromatography with the mixture of petroleum ether and dichloromethane (1:2, v/v) as the eluent, yielding a dark brown solid (275 mg, 95%). ¹H NMR (400 MHz, Chloroform-*d*) δ 9.03 (s, 2H), 8.53 (dd, *J* = 10.0, 6.4 Hz, 2H), 7.65 (t, *J* = 7.5 Hz, 2H),

6.42 (d, $J = 10.7$ Hz, 4H), 4.39 (hept, $J = 5.9$ Hz, 4H), 3.11 – 2.93 (m, 4H), 1.68 (p, $J = 7.6$ Hz, 4H), 1.37 – 1.21 (m, 20H), 1.18 (d, $J = 6.0$ Hz, 12H), 1.02 (d, $J = 6.0$ Hz, 12H), 0.87 (t, $J = 6.8$ Hz, 6H). MS (MALDI-TOF): m/z 1540.60



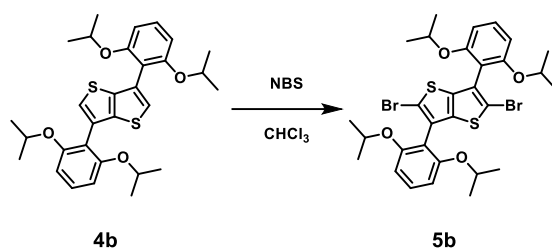
Compound 2b:

To a solution of Compound 1b (6000 mg, 30.88 mmol) in 40 mL dry Et₂O, N,N,N',N'-tetramethylethylenediamine (TMEDA) (3.8 mL) and *n*-BuLi (16.8 mL, 2.4 M, 40.32 mmol) was added dropwise under the protection of argon at -5 °C. After the mixture was stirred at -5 °C for 1 h, 40 mL THF was injected. Then, B(OCH₃)₃ (6418 mg, 61.74 mmol) was injected at -78 °C and the mixture was allowed to warm up to room temperature gradually. After quenched with 100 mL 1 M HCl, the mixture was stirred for 3 h and then extracted with dichloromethane. The combined organic phase was evaporated under vacuum. The obtained product was used directly in the next reaction without further purification, yielding a colorless oil (6985 mg, 95%). ¹H NMR (400 MHz, Chloroform-*d*) δ 7.51 (s, 2H), 7.32 (t, $J = 8.4$ Hz, 1H), 6.59 (d, $J = 8.4$ Hz, 2H), 4.69 (hept, $J = 6.1$ Hz, 2H), 1.40 (d, $J = 6.1$ Hz, 12H).



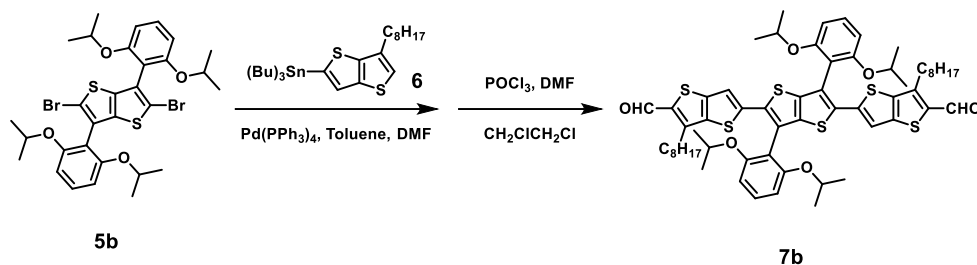
Compound 4b:

Compound 3 (600 mg, 2.01 mmol), Compound 2b (1917 mg, 8.05 mmol), and potassium phosphate tribasic (K₃PO₄) (2987 mg, 14.07 mmol) were added in toluene (30 mL). The mixture was frozen by liquid nitrogen, followed by three times of successive vacuum and argon fill cycles. Then, Pd₂(dba)₃ (110 mg, 0.12 mmol) and 2-dicyclohexylphosphino-2',6'-dimethoxybiphenyl (S-Phos) (99 mg, 0.24 mmol) were added and another three times of successive vacuum and argon fill cycles were performed. The mixture was refluxed at 110 °C for 48 h. After pouring into the water, the mixture was extracted with dichloromethane. The combined organic phase was evaporated under vacuum. The obtained crude product was purified through column chromatography with the mixture of petroleum ether and dichloromethane (1:1, v/v) to afford Compound 4b as a white solid (886 mg, 84%). ¹H NMR (400 MHz, Chloroform-*d*) δ 7.33 (s, 2H), 7.22 (t, $J = 8.3$ Hz, 2H), 6.68 (d, $J = 8.3$ Hz, 4H), 4.28 (hept, $J = 6.0$ Hz, 4H), 1.15 (d, $J = 6.1$ Hz, 24H).



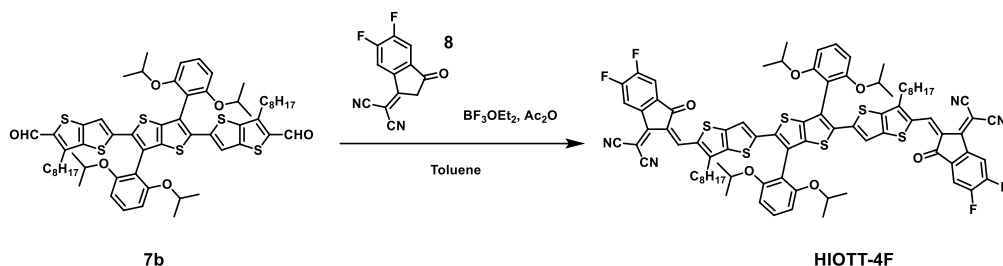
Compound 5b:

To a solution of compound 4b (600 mg, 1.14 mmol) in 20 mL CHCl_3 , N-succinbromimide (NBS) (417 mg, 2.34 mmol) was added and stirred dark at 0 °C for about 10 min (monitored by TLC). After the solvent was evaporated, methanol was added and filtered. The product was dried in vacuum to yield a white solid (763 mg, 98%). $^1\text{H NMR}$ (400 MHz, Chloroform-*d*) δ 7.29 (t, $J = 8.3$ Hz, 2H), 6.66 (d, $J = 8.3$ Hz, 4H), 4.30 (hept, $J = 6.1$ Hz, 4H), 1.16 (dd, $J = 7.7, 6.2$ Hz, 24H).



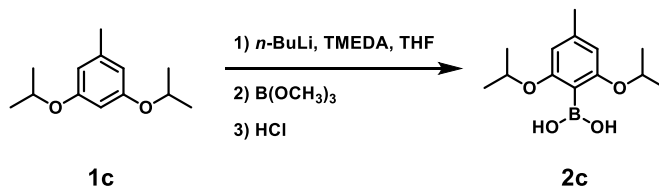
Compound 7b:

Compound 5b (600 mg, 0.88 mmol) and Compound 6 (1190 mg, 2.20 mmol) were dissolved in toluene (20 mL) and DMF (5 mL). The mixture was frozen by liquid nitrogen, followed by three times of successive vacuum and argon fill cycles. Then, $\text{Pd}(\text{PPh}_3)_4$ (61 mg, 0.05 mmol) was added and another three times of successive vacuum and argon fill cycles were performed. The mixture was refluxed at 120 °C overnight. After cooling to room temperature, the mixture was diluted with petroleum ether and quickly passed through a silica gel column with dichloromethane as the eluent. After the solvent was removed by rotary evaporation, the mixture was dissolved with 1,2-dichloroethane and injected into the Vilsmeier-Haack reagent (freshly prepared by 0.5 mL POCl_3 and 1 mL DMF at 0 °C under argon). The mixture was heated to 70 °C and kept for about 2 h (monitored by TLC). After cooling to room temperature, the mixture was poured slowly into a saturated sodium bicarbonate solution and stirred for another 4 h. The crude product was extracted with dichloromethane and dried over anhydrous Na_2SO_4 . After removing the solvent, silica gel column chromatography was used to purify the product with the mixture of petroleum ether and dichloromethane (1:1~1:4, v/v) as the eluent, yielding an orange solid (695 mg, 73% in total). $^1\text{H NMR}$ (400 MHz, Chloroform-*d*) δ 10.00 (s, 2H), 7.36 (t, $J = 8.3$ Hz, 2H), 7.09 (s, 2H), 6.67 (d, $J = 8.4$ Hz, 4H), 4.35 (hept, $J = 6.0$ Hz, 4H), 2.98 (t, $J = 7.3$ Hz, 4H), 1.69 (p, $J = 7.4$ Hz, 4H), 1.30 – 1.22 (m, 20H), 1.14 (d, $J = 6.0$ Hz, 12H), 0.99 (d, $J = 6.0$ Hz, 12H), 0.88 (t, $J = 6.8$ Hz, 6H).



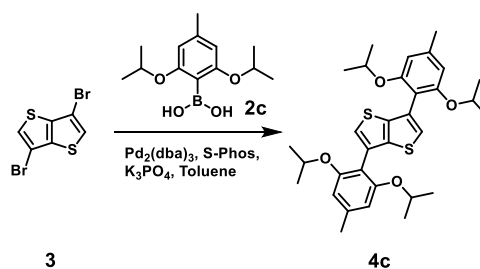
HIOTT-4F:

HIOTT-4F was prepared by the method from the literature report⁴. Compound 7b (200 mg, 0.18 mmol) and Compound 8 (94 mg, 0.41 mmol) were dissolved in toluene (20 mL). Then, BF_3OEt_2 (319 mg, 2.25 mmol) and Ac_2O (0.2 mL) was injected and the mixture was stirring at room temperature for 1 h. Once the reaction was completed, the mixture was poured into methanol and the filtered solid was purified by silica gel column chromatography with the mixture of petroleum ether and dichloromethane (1:2, v/v) as the eluent, yielding a dark brown solid (258 mg, 95%). ^1H NMR (400 MHz, Chloroform-*d*) δ 9.01 (s, 2H), 8.53 (dd, $J = 10.0, 6.5$ Hz, 2H), 7.64 (t, $J = 7.5$ Hz, 2H), 7.42 (t, $J = 8.4$ Hz, 2H), 7.14 (s, 2H), 6.70 (d, $J = 8.4$ Hz, 4H), 4.40 (hept, $J = 6.1$ Hz, 4H), 3.10 – 2.90 (m, 4H), 1.67 (p, $J = 8.1, 6.8$ Hz, 4H), 1.35 – 1.22 (m, 20H), 1.16 (d, $J = 6.0$ Hz, 12H), 1.02 (d, $J = 6.0$ Hz, 12H), 0.88 (t, $J = 6.8$ Hz, 6H). MS (MALDI-TOF): m/z 1504.75



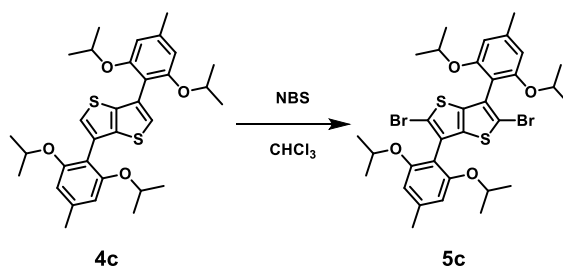
Compound 2c:

To a solution of Compound 1c (3516 mg, 16.88 mmol) in 20 mL dry Et_2O , N,N,N',N' -tetramethylethylenediamine (TMEDA) (2.1 mL) and $n\text{-BuLi}$ (9.2 mL, 2.4 M, 21.94 mmol) was added dropwise under the protection of argon at -5 °C. After the mixture was stirred at -5 °C for 1 h, 20 mL THF was injected. Then, $\text{B}(\text{OCH}_3)_3$ (3508 mg, 33.76 mmol) was injected at -78 °C and the mixture was allowed to warm up to room temperature gradually. After quenched with 100 mL 1 M HCl, the mixture was stirred for 3 h and then extracted with dichloromethane. The combined organic phase was evaporated under vacuum. The obtained product was used directly in the next reaction without further purification, yielding a colorless oil (3830 mg, 90%). ^1H NMR (400 MHz, Chloroform-*d*) δ 7.45 (s, 2H), 6.40 (s, 2H), 4.68 (hept, $J = 6.1$ Hz, 2H), 2.33 (s, 3H), 1.39 (d, $J = 6.1$ Hz, 12H).



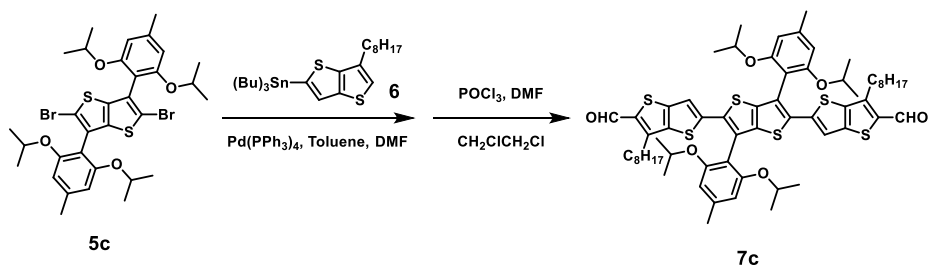
Compound 4c:

Compound 3 (608 mg, 2.04 mmol), Compound 2c (2058 mg, 8.16 mmol), and potassium phosphate tribasic (K₃PO₄) (3031 mg, 14.28 mmol) were added in toluene (30 mL). The mixture was frozen by liquid nitrogen, followed by three times of successive vacuum and argon fill cycles. Then, Pd₂(dba)₃ (110 mg, 0.12 mmol) and 2-dicyclohexylphosphino-2',6'-dimethoxybiphenyl (S-Phos) (98 mg, 0.24 mmol) were added and another three times of successive vacuum and argon fill cycles were performed. The mixture was refluxed at 110 °C for 48 h. After pouring into the water, the mixture was extracted with dichloromethane. The combined organic phase was evaporated under vacuum. The obtained crude product was purified through column chromatography with the mixture of petroleum ether and dichloromethane (1:1, v/v) to afford Compound 4c as a white solid (925 mg, 82%). ¹H NMR (400 MHz, Chloroform-*d*) δ 7.29 (s, 2H), 6.51 (s, 4H), 4.24 (hept, *J* = 6.0 Hz, 4H), 2.37 (s, 6H), 1.13 (d, *J* = 6.1 Hz, 24H).



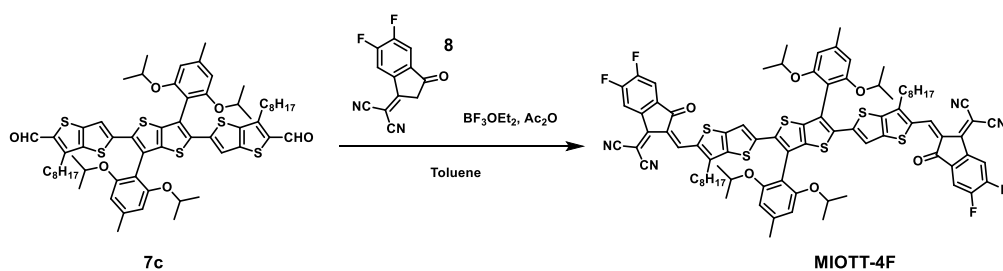
Compound 5c:

To a solution of compound 4c (800 mg, 1.45 mmol) in 20 mL CHCl₃, N-succinbromimide (NBS) (528 mg, 2.97 mmol) was added and stirred dark at 0 °C for about 10 min (monitored by TLC). After the solvent was evaporated, methanol was added and filtered. The product was dried in vacuum to yield a white solid (979 mg, 95%). ¹H NMR (400 MHz, Chloroform-*d*) δ 6.48 (s, 4H), 4.26 (hept, *J* = 6.1 Hz, 4H), 2.38 (s, 6H), 1.17 – 1.10 (m, 24H).



Compound 7c:

Compound 5c (927 mg, 1.30 mmol) and Compound 6 (1766 mg, 3.26 mmol) were dissolved in toluene (20 mL) and DMF (5 mL). The mixture was frozen by liquid nitrogen, followed by three times of successive vacuum and argon fill cycles. Then, Pd(PPh₃)₄ (90 mg, 0.08 mmol) was added and another three times of successive vacuum and argon fill cycles were performed. The mixture was refluxed at 120 °C overnight. After cooling to room temperature, the mixture was diluted with petroleum ether and quickly passed through a silica gel column with dichloromethane as the eluent. After the solvent was removed by rotary evaporation, the mixture was dissolved with 1,2-dichloroethane and injected into the Vilsmeier-Haack reagent (freshly prepared by 0.8 mL POCl₃ and 1.5 mL DMF at 0 °C under argon). The mixture was heated to 70 °C and kept for about 2 h (monitored by TLC). After cooling to room temperature, the mixture was poured slowly into a saturated sodium bicarbonate solution and stirred for another 4 h. The crude product was extracted with dichloromethane and dried over anhydrous Na₂SO₄. After removing the solvent, silica gel column chromatography was used to purify the product with the mixture of petroleum ether and dichloromethane (1:1~1:4, v/v) as the eluent, yielding an orange solid (980 mg, 68% in total). ¹H NMR (400 MHz, Chloroform-*d*) δ 10.00 (s, 2H), 7.09 (s, 2H), 6.50 (s, 4H), 4.32 (hept, *J* = 6.1 Hz, 4H), 2.99 (t, *J* = 6.7 Hz, 4H), 2.44 (s, 6H), 1.70 (p, *J* = 6.8 Hz, 4H), 1.32 – 1.21 (m, 20H), 1.12 (d, *J* = 6.0 Hz, 12H), 0.98 (d, *J* = 6.0 Hz, 12H), 0.87 (t, *J* = 6.8 Hz, 6H).



MIOTT-4F:

MIOTT-4F was prepared by the method from the literature report⁴. Compound 7c (250 mg, 0.23 mmol) and Compound 8 (114 mg, 0.50 mmol) were dissolved in toluene (20 mL). Then, BF₃OEt₂ (399 mg, 2.81 mmol) and Ac₂O (0.3 mL) was injected and the mixture was stirring at room temperature for 1 h. Once the reaction was completed, the mixture was poured into methanol and the filtered solid was purified by silica gel column chromatography with the mixture of petroleum ether and dichloromethane (1:2, v/v) as the eluent, yielding a dark brown solid (335 mg, 95%). ¹H NMR (400 MHz, Chloroform-*d*) δ 9.01 (s, 2H), 8.52 (dd, *J* = 10.0, 6.4 Hz, 2H), 7.63 (t, *J* = 7.5 Hz, 2H), 7.14 (s, 2H), 6.52 (s, 4H), 4.37 (hept, *J* = 6.0 Hz, 4H), 3.02 (t, *J* = 7.6 Hz, 4H), 2.47 (s, 6H), 1.68 (p, *J* = 7.5 Hz, 4H), 1.35 – 1.21 (m, 20H), 1.14 (d, *J* = 6.0 Hz, 12H), 1.00 (d, *J* = 6.0 Hz, 12H), 0.87 (t, *J* = 6.8 Hz, 6H). MS (MALDI-TOF): *m/z* 1532.65

Supplementary NMR Figures

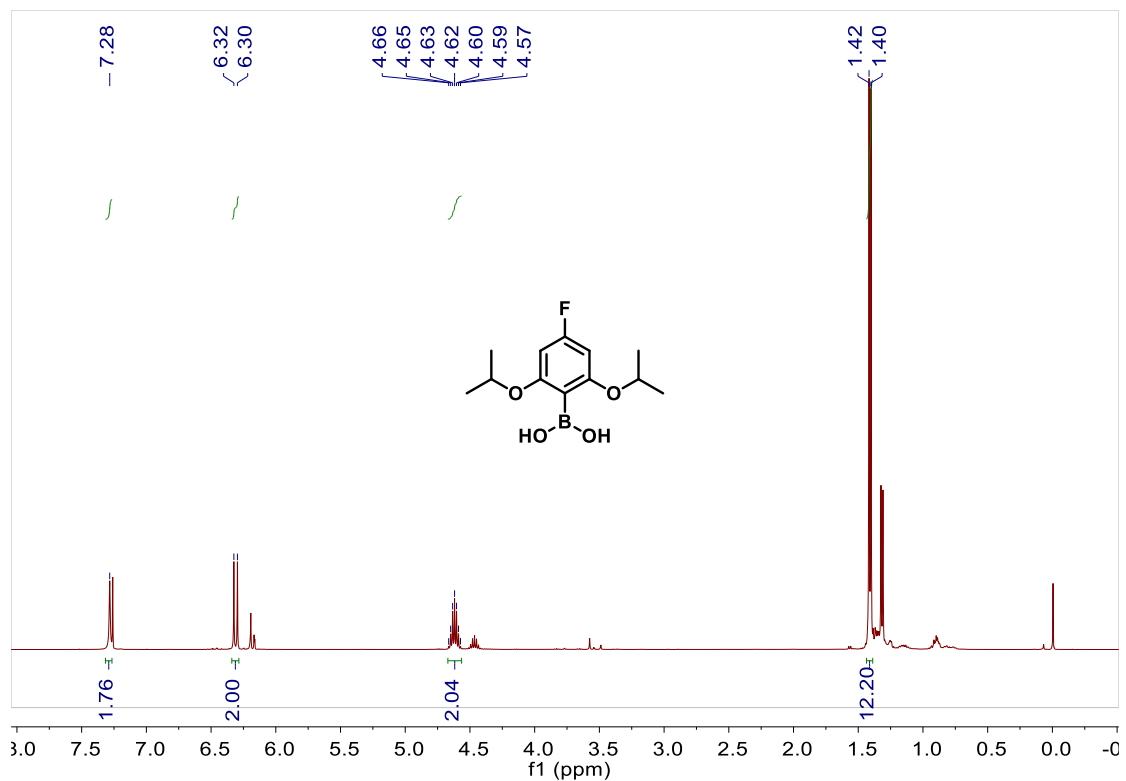


Fig. S1 ¹H-NMR spectrum of compound 2a.

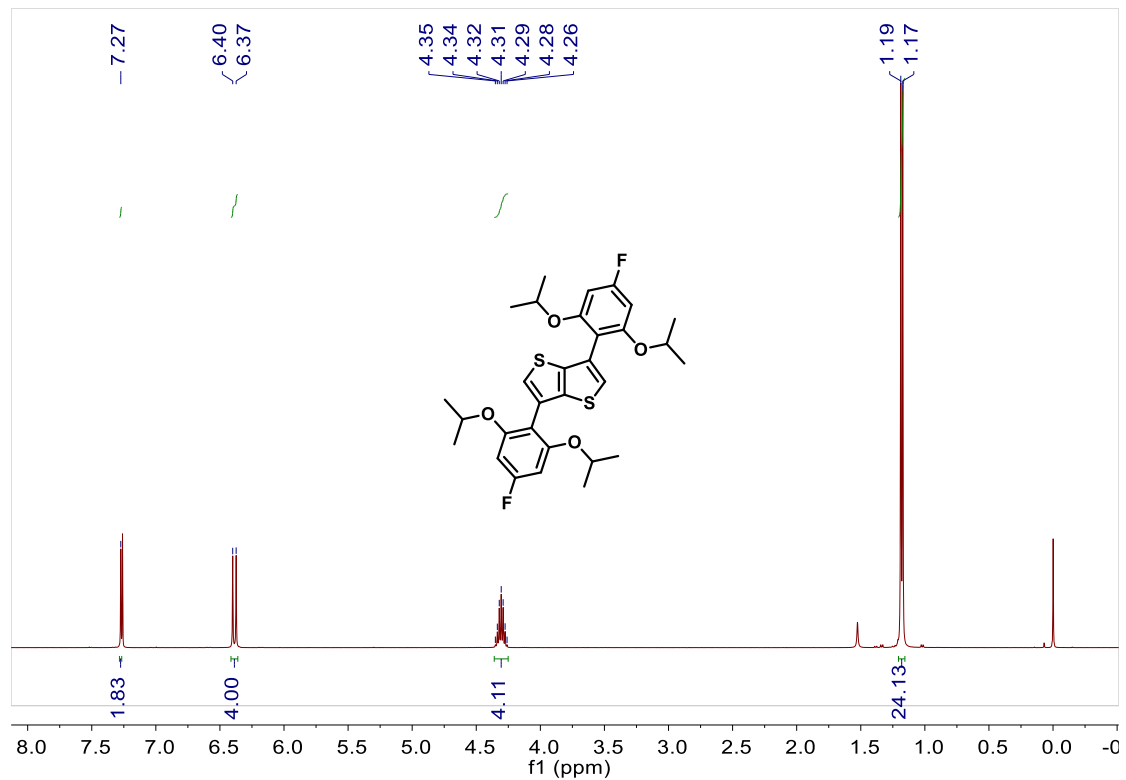


Fig. S2 ¹H-NMR spectrum of compound 4a.

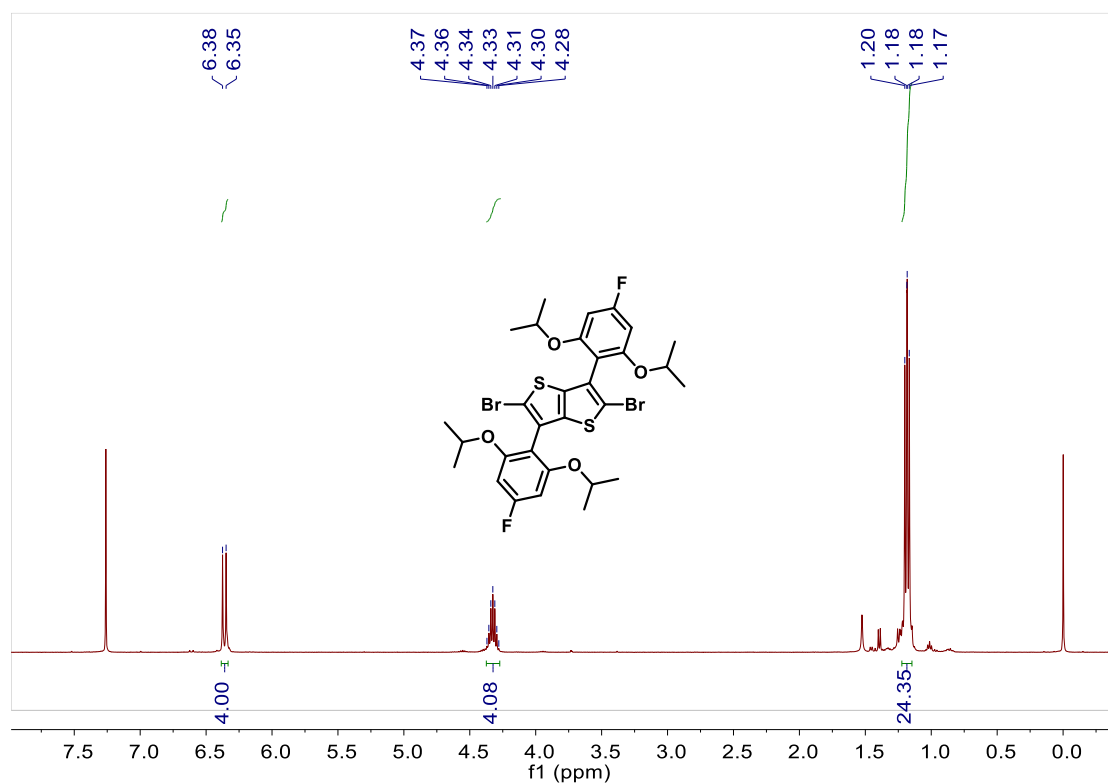


Fig. S3 $^1\text{H-NMR}$ spectrum of compound 5a.

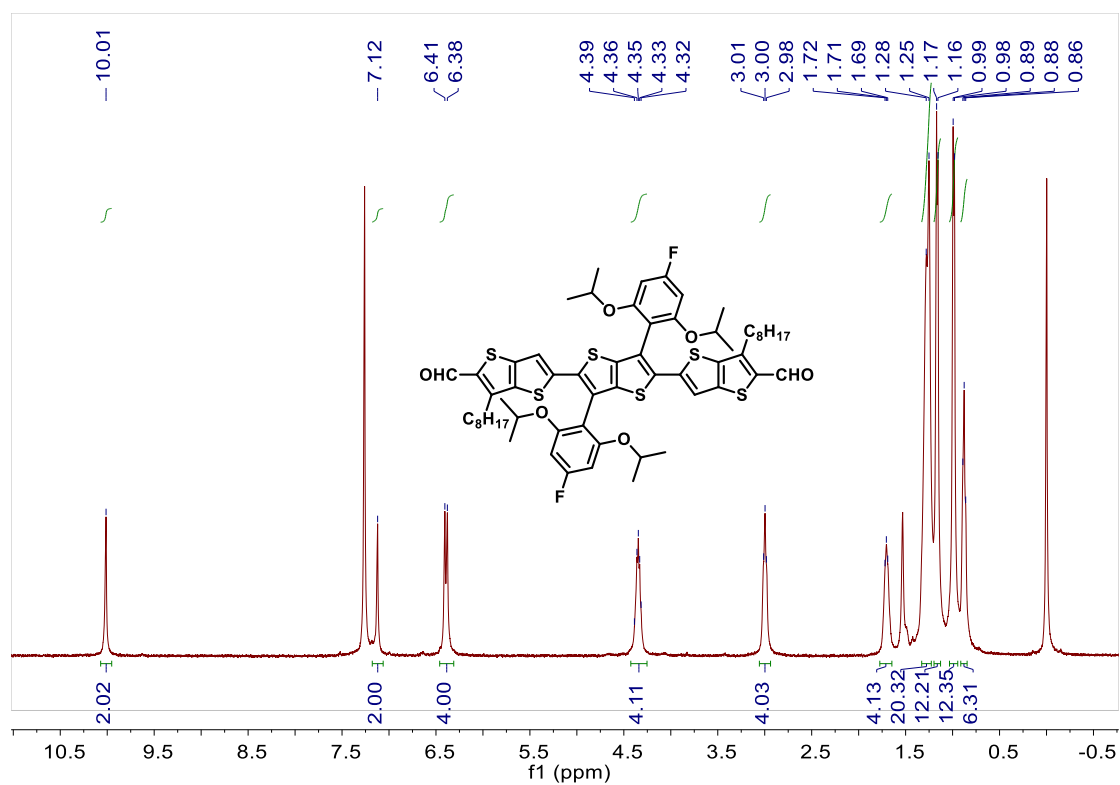


Fig. S4 $^1\text{H-NMR}$ spectrum of compound 7a.

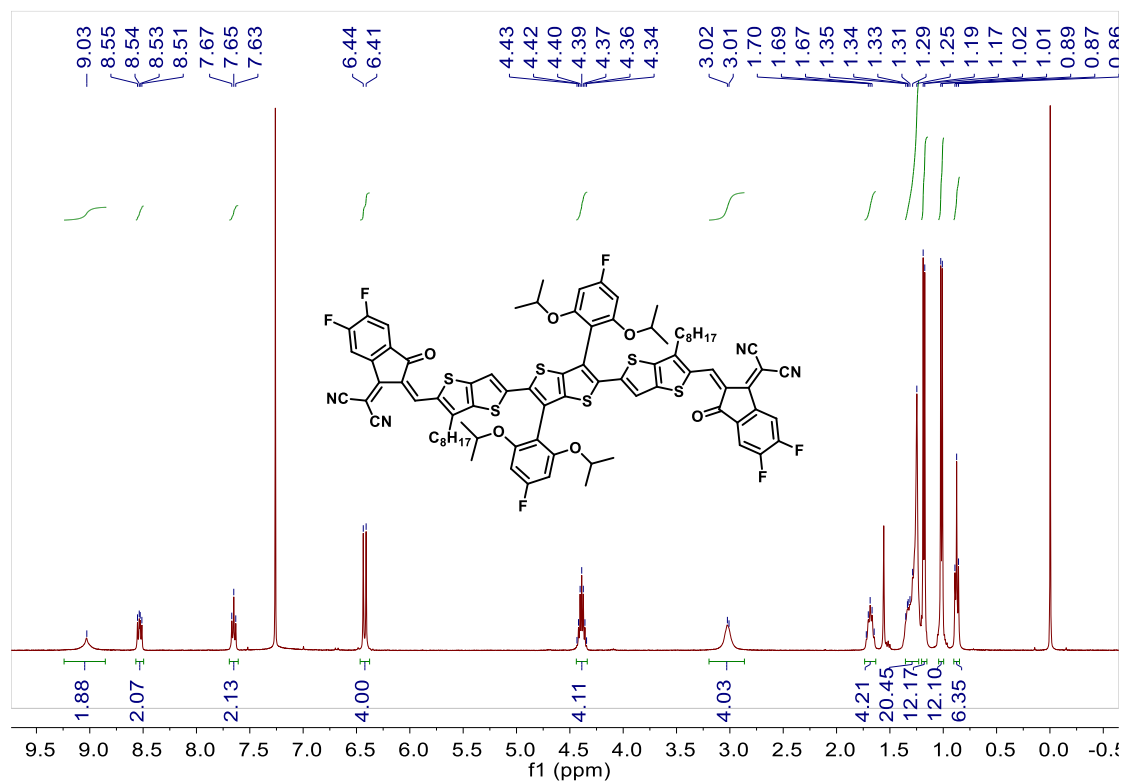


Fig. S5 ¹H-NMR spectrum of FIOTT-4F.

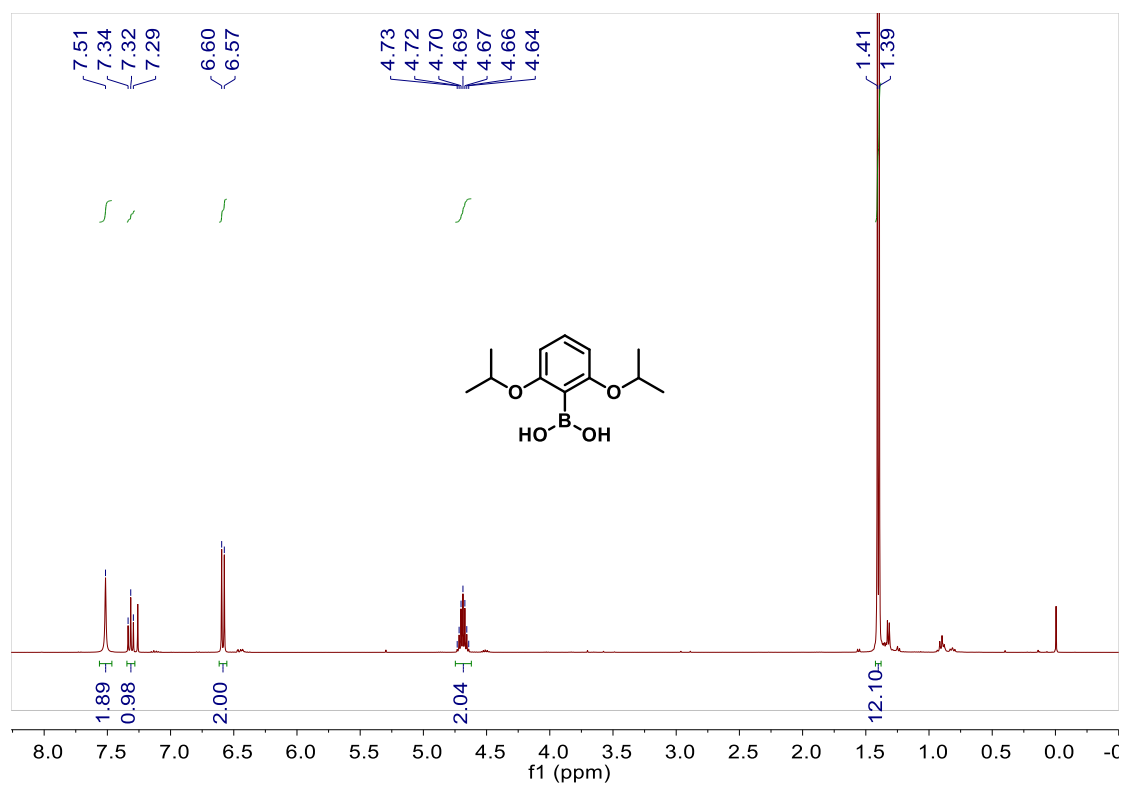


Fig. S6 ¹H-NMR spectrum of compound 2b.

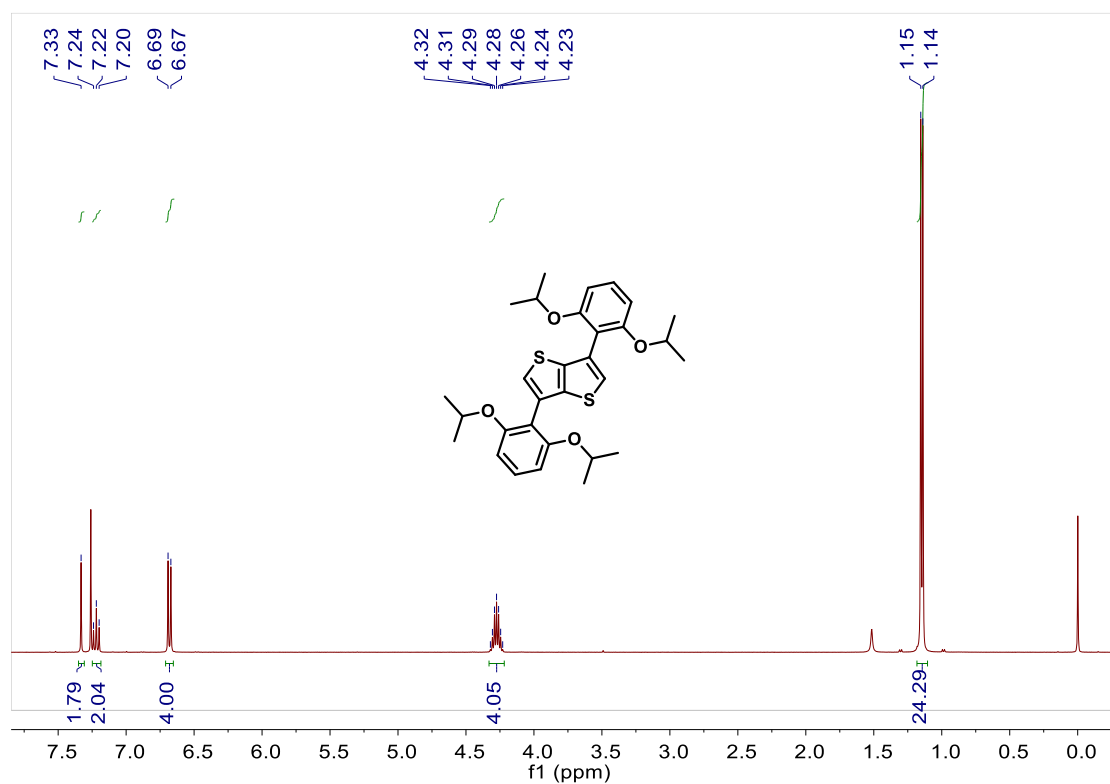


Fig. S7 $^1\text{H-NMR}$ spectrum of compound 4b.

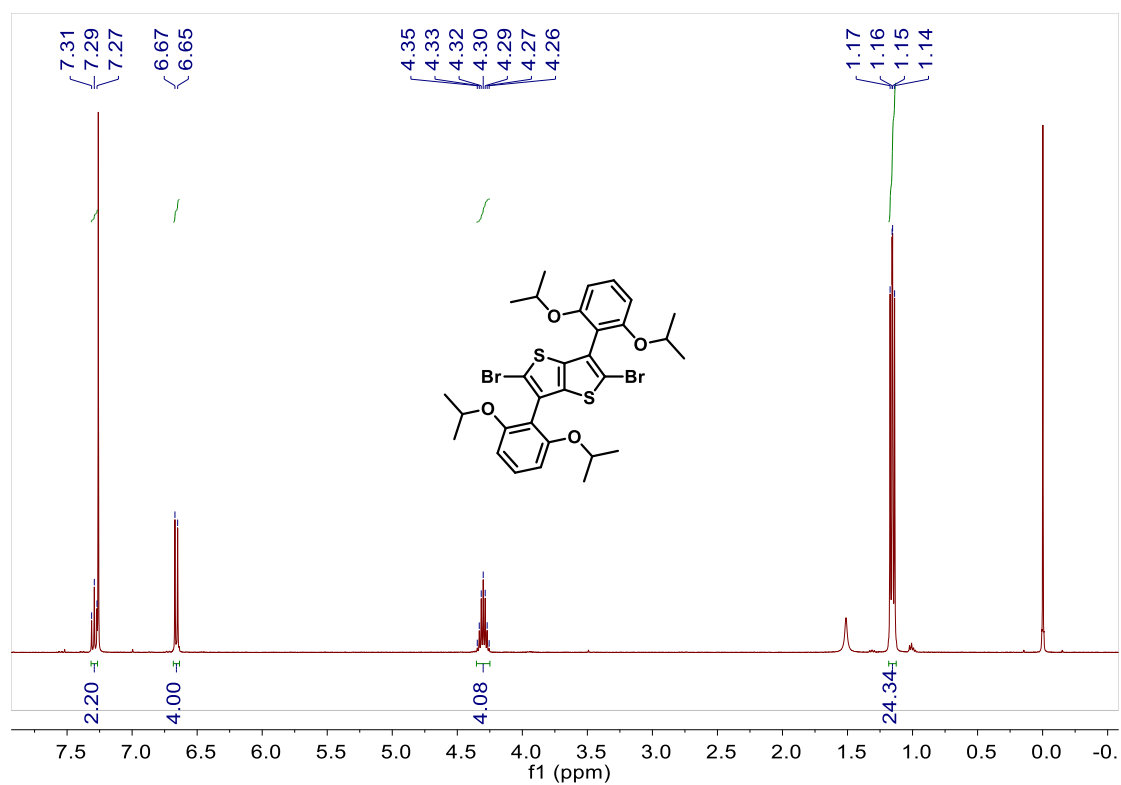


Fig. S8 $^1\text{H-NMR}$ spectrum of compound 5b.

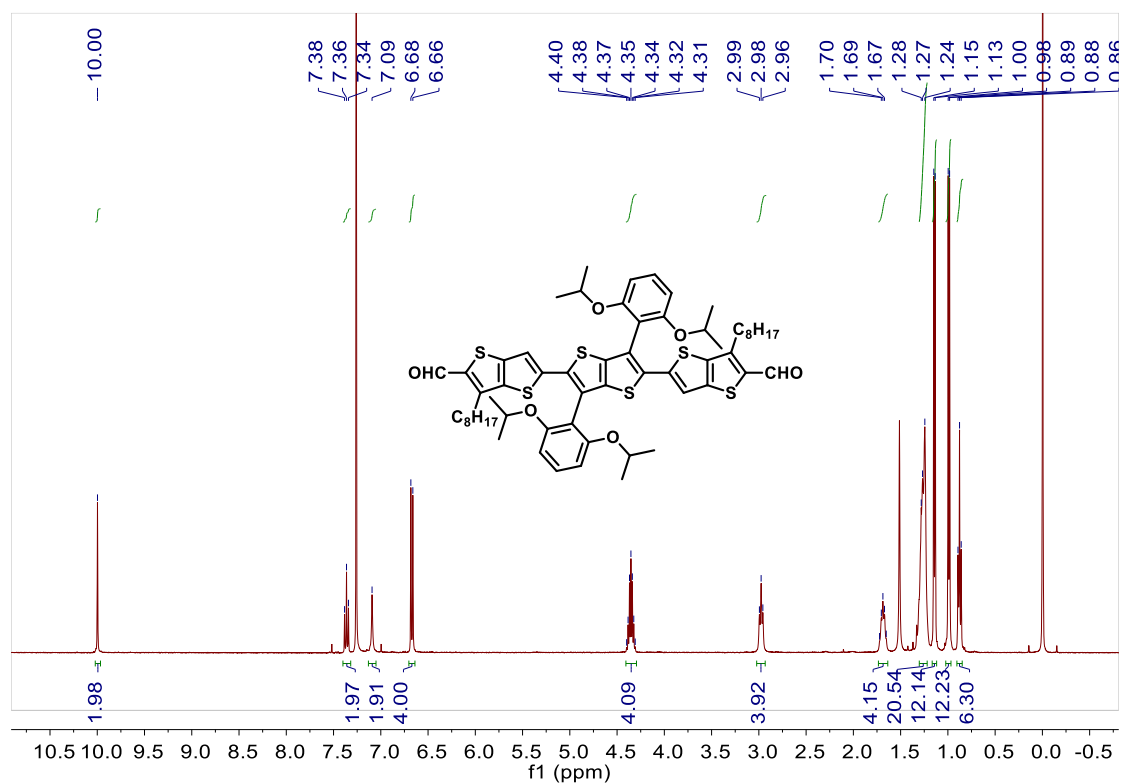


Fig. S9 $^1\text{H-NMR}$ spectrum of compound 7b.

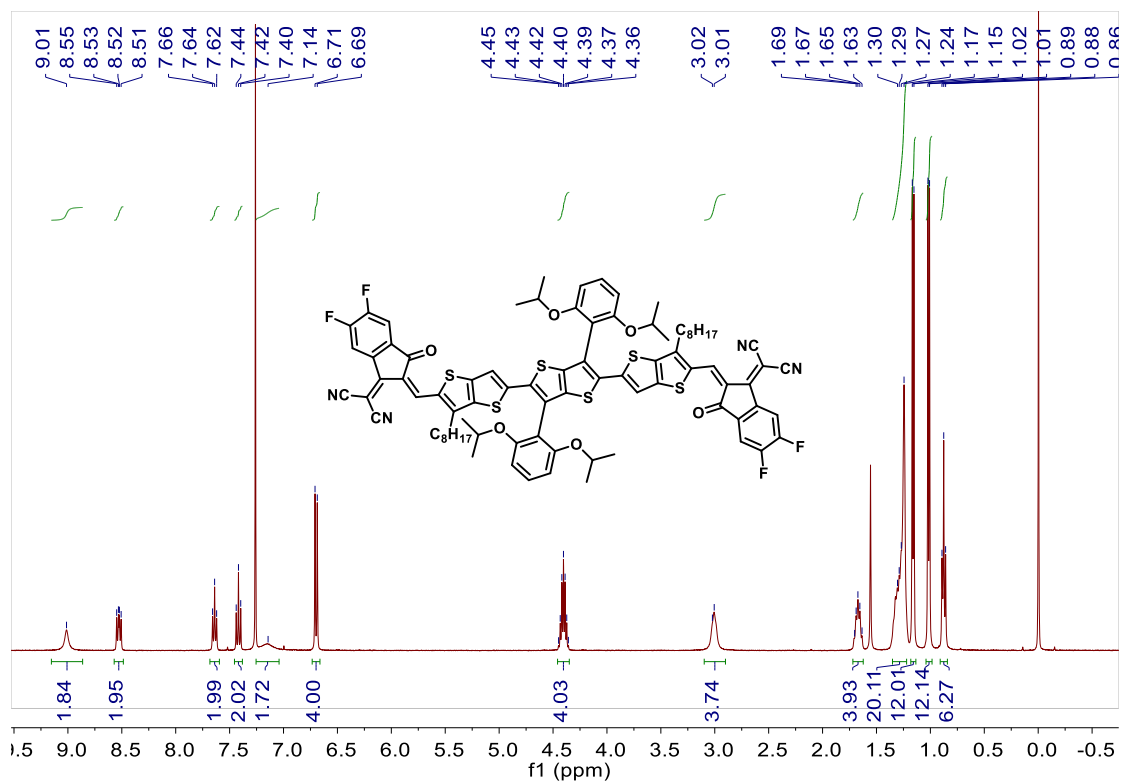


Fig. S10 $^1\text{H-NMR}$ spectrum of HIOTT-4F.

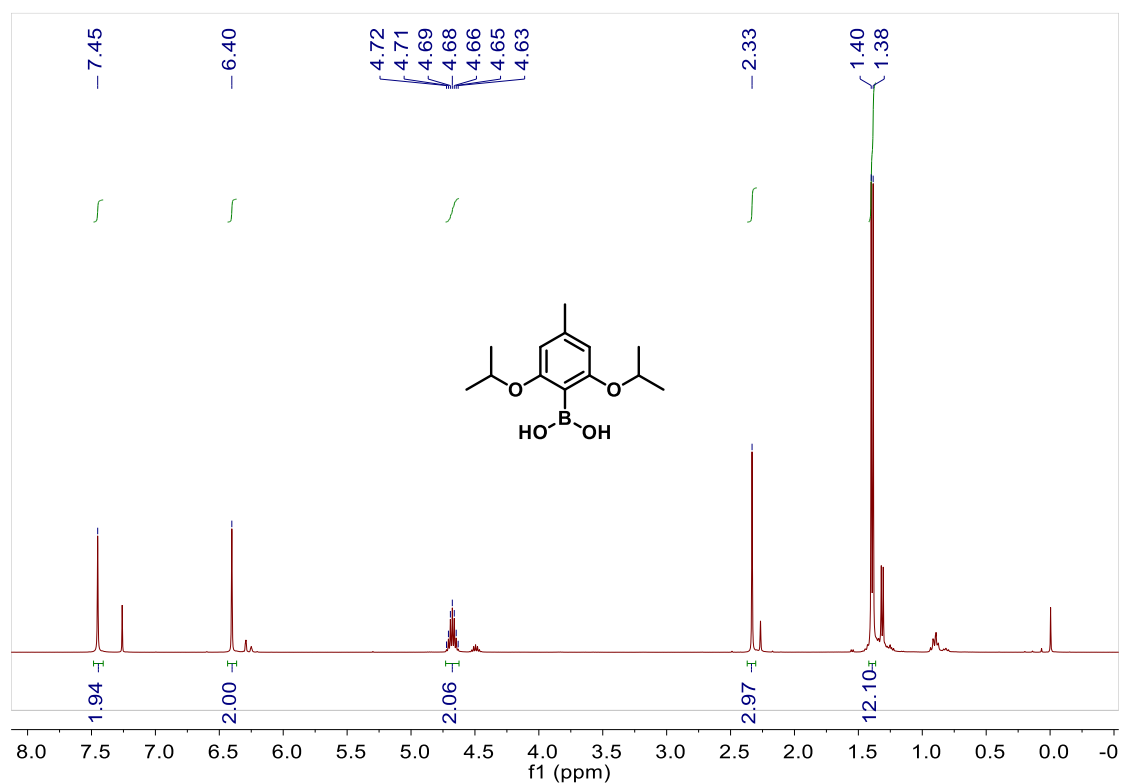


Fig. S11 $^1\text{H-NMR}$ spectrum of compound 2c.

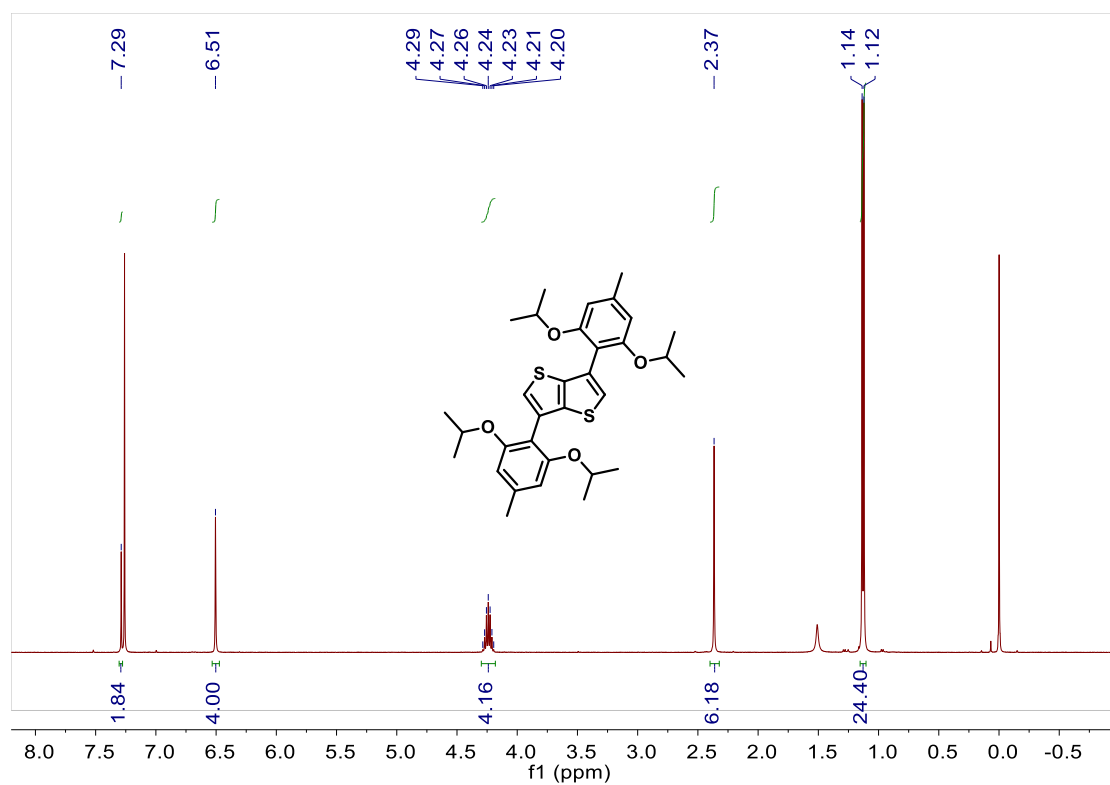


Fig. S12 $^1\text{H-NMR}$ spectrum of compound 4c.

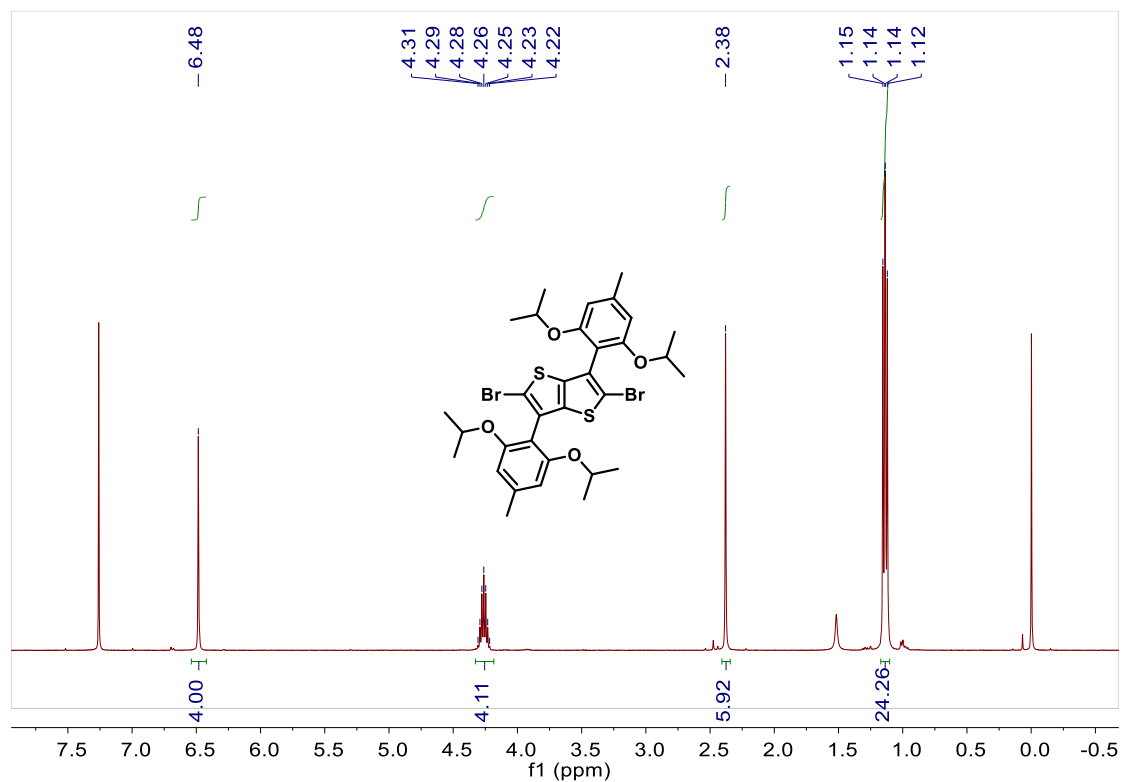


Fig. S13 $^1\text{H-NMR}$ spectrum of compound 5c.

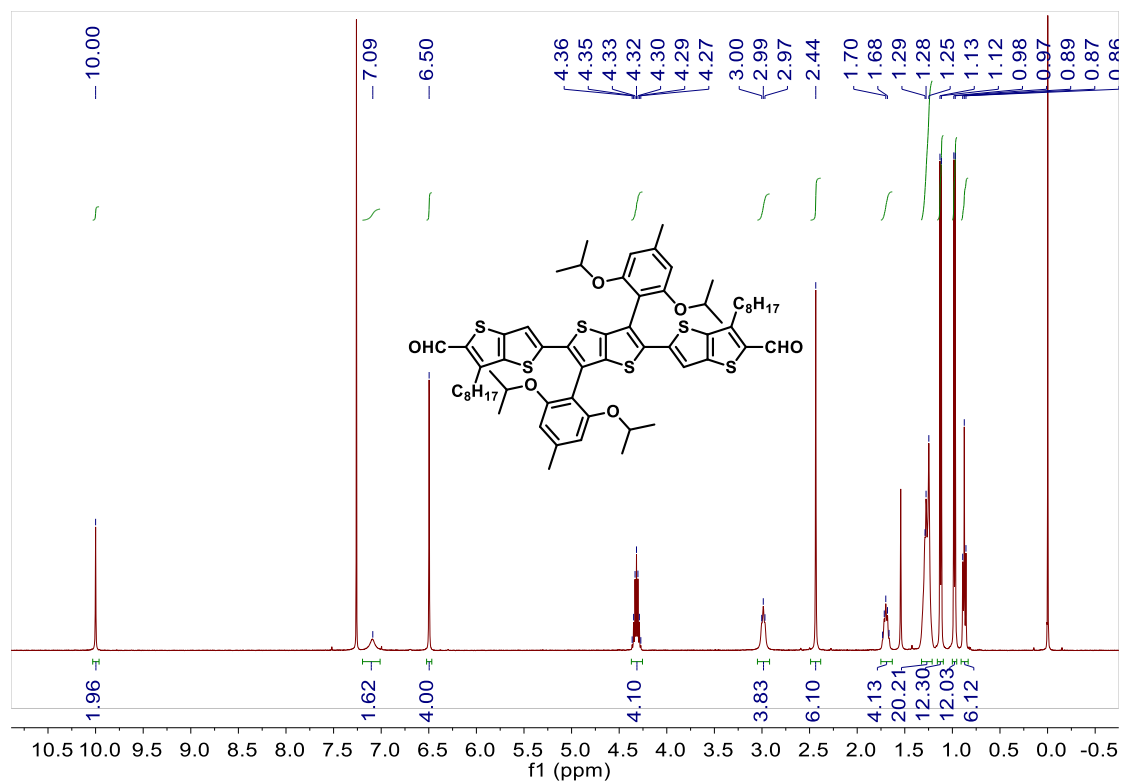


Fig. S14 $^1\text{H-NMR}$ spectrum of compound 7c.

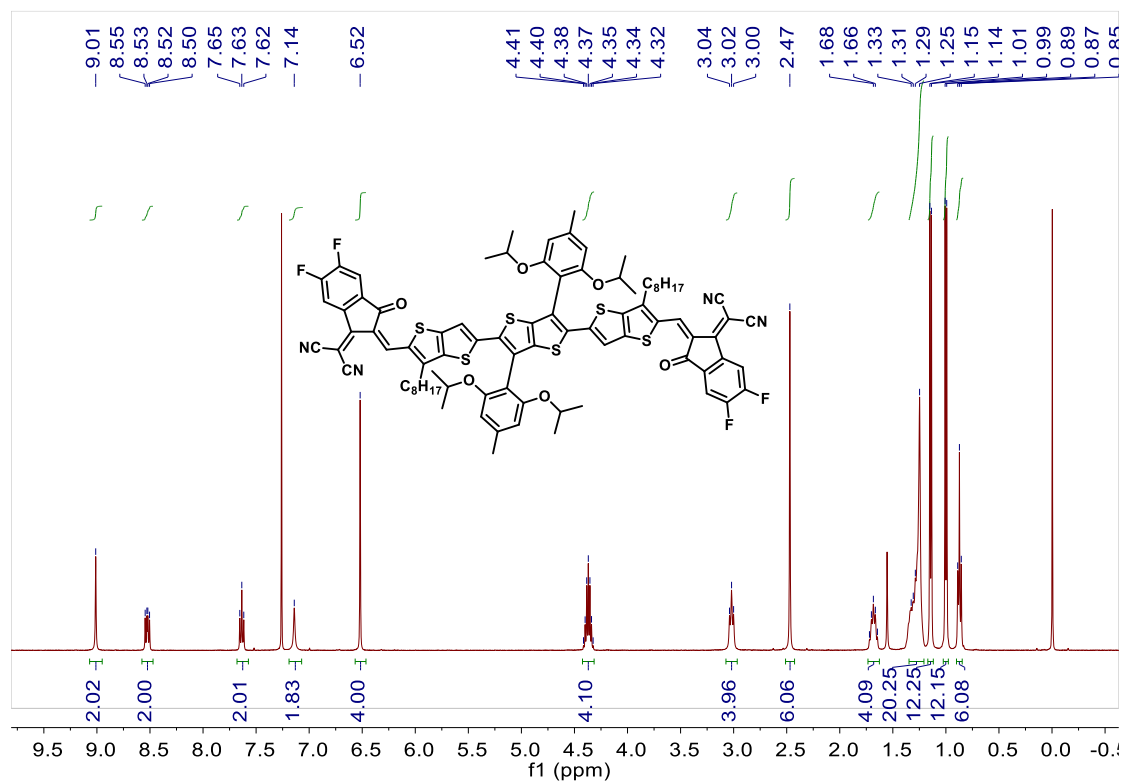


Fig. S15 ¹H-NMR spectrum of MIOTT-4F.

Supplementary MALDI-TOF Figures

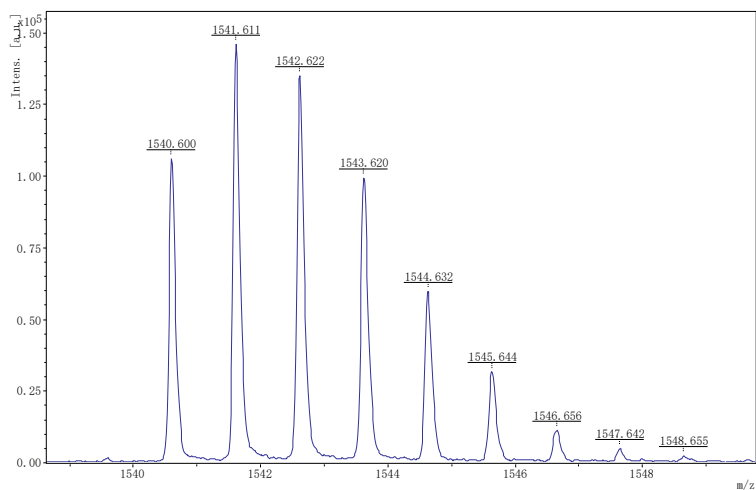


Fig. S16 MALDI-TOF mass spectrum of FIOTT-4F.

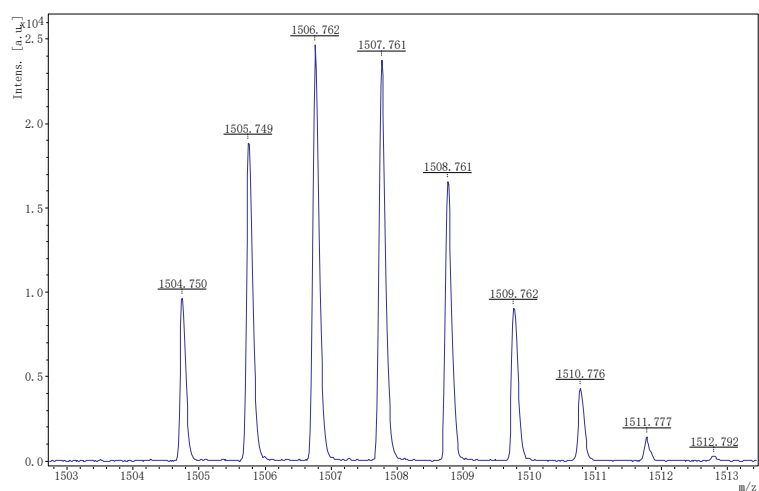


Fig. S17 MALDI-TOF mass spectrum of HIOTT-4F.

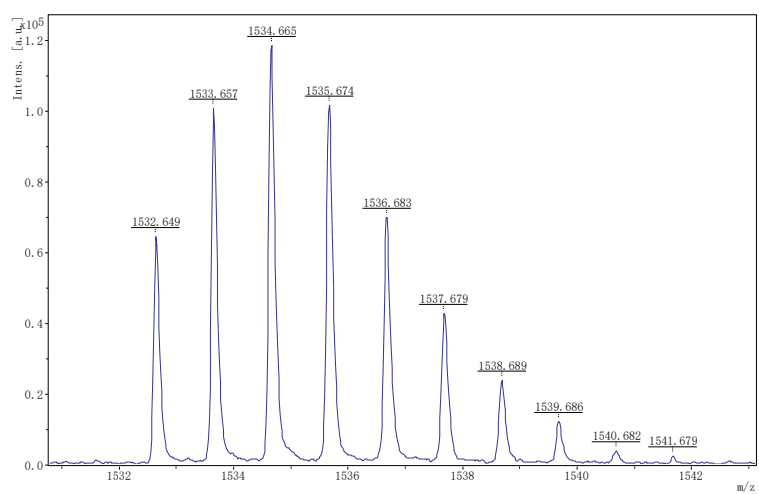


Fig. S18 MALDI-TOF mass spectrum of MIOTT-4F.

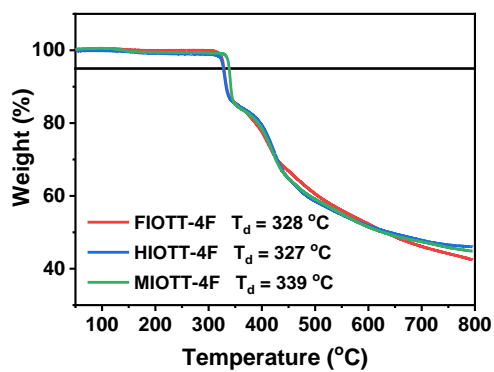


Fig. S19 TGA curves of the acceptors.

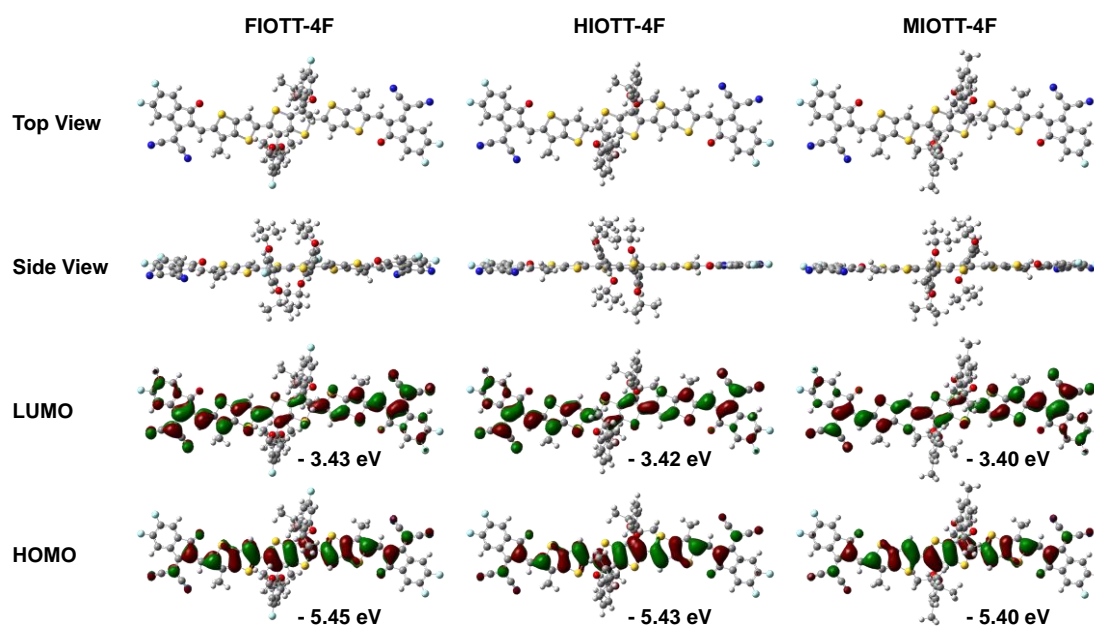


Fig. S20 Optimized molecular geometries and frontier molecular orbitals of the acceptors with simplified side chains calculated by density functional theory.

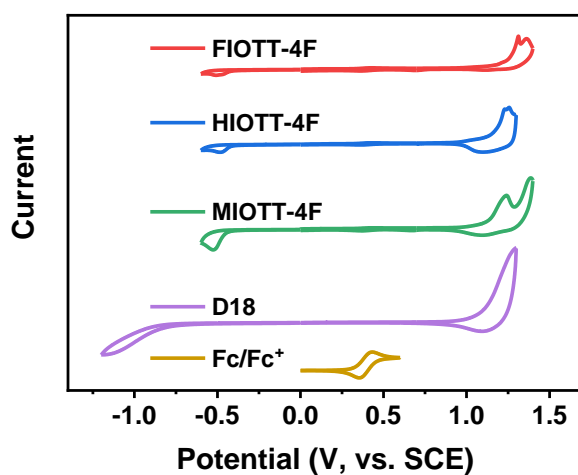


Fig. S21 Cyclic voltammograms of FIOTT-4F, HIOTT-4F, MIOTT-4F, D18 and Fc/Fc⁺ in acetonitrile solutions.

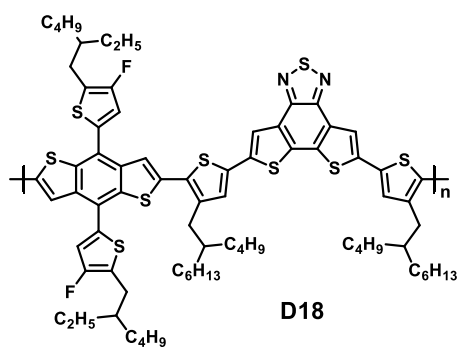


Fig. S22 Chemical structure of D18.

Table S1 Crystal data and structure refinement for the three acceptors.

	FIOTT-4F	HIOTT-4F	MIOTT-4F
CCDC Deposition Number	2353971	2353972	2353973
Chemical formula (moiety)	C ₈₄ H ₇₄ F ₆ N ₄ O ₆ S ₆	C ₈₄ H ₇₅ F ₄ N ₄ O ₆ S ₆ , C ₄₂ H ₃₈ F ₂ N ₂ O ₃ S ₃	2(C ₄₃ H ₄₀ F ₂ N ₂ O ₃ S ₃)
Chemical formula (sum)	C ₈₄ H ₇₄ F ₆ N ₄ O ₆ S ₆	C ₁₂₆ H ₁₁₃ F ₆ N ₆ O ₉ S ₉	C ₈₆ H ₈₀ F ₄ N ₄ O ₆ S ₆
Chemical formula weight	1541.83	2257.76	1533.90
Temperature [K]	170(2)	170(2)	170(2)
Crystal system	Monoclinic	Triclinic	Triclinic
Space group	P 1 21/c 1	P -1	P -1
a [Å]	20.4033(9)	15.5739(12)	15.606(3)
b [Å]	7.8689(3)	18.8499(15)	16.678(3)
c [Å]	25.4607(12)	20.1648(13)	18.394(3)
α [°]	90	98.961(5)	63.176(11)
β [°]	91.450(2)	96.362(4)	69.390(14)
γ [°]	90	98.914(5)	69.980(15)
Volume [Å ³]	4086.4(3)	5721.3(7)	3901.2(13)
Z	2	2	2
ρ _{calc} [g cm ⁻³]	1.253	1.311	1.306
Absorpt coefficient [mm ⁻¹]	2.101	2.199	2.159
F(000)	1608	2362	1608
θ range [°]	2.166 to 66.596	2.240 to 66.594	2.770 to 54.235
Reflections collected	34671	63824	18373
Independent reflections	7187	20079	8683
Data/restraints/parameters	7187/98/538	20079/234/1408	8683/414/931
Goodness-of-fit on F ²	1.050	1.204	1.060
R1, wR2 [I ≥ 2σ (I)]	0.0821, 0.2414	0.1847, 0.4266	0.1800, 0.4130
R1, wR2 [all data]	0.0877, 0.2464	0.2413, 0.4694	0.2701, 0.4989
Largest diff. peak/hole [e Å ⁻³]	1.481/-0.426	1.157/-0.839	0.494/-0.393

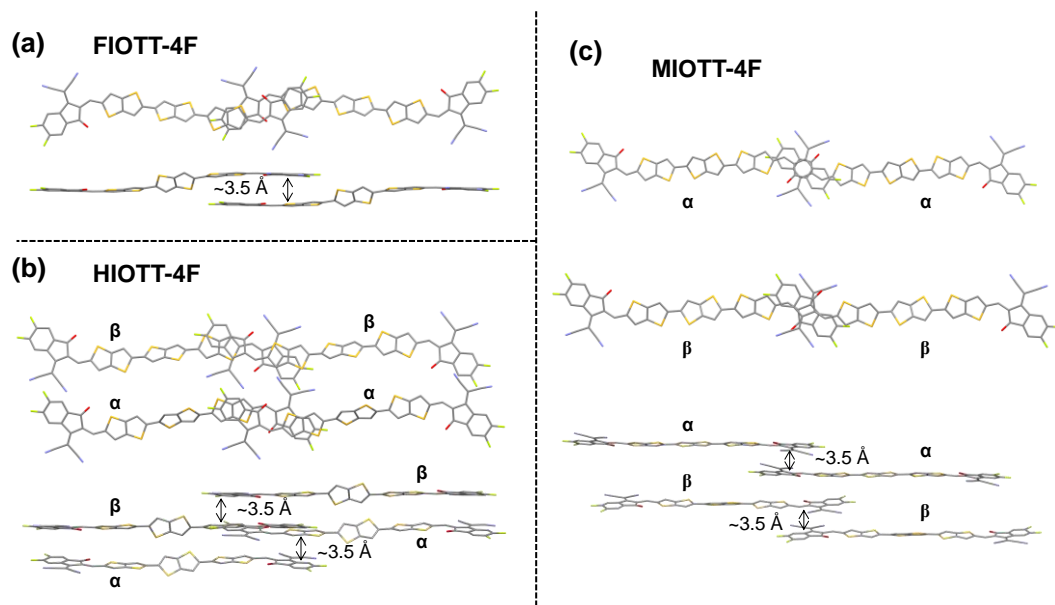


Fig. S23 The π - π stacking distances in a) FIOTT-4F, b) HIOTT-4F, and c) MIOTT-4F single crystals.

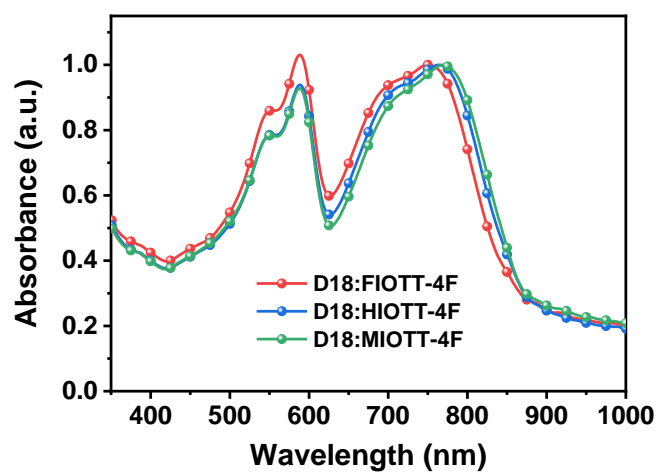


Fig. S24 UV-vis absorption spectra of D18:FIOTT-4F, D18:HIOTT-4F and D18:MIOTT-4F blend films.

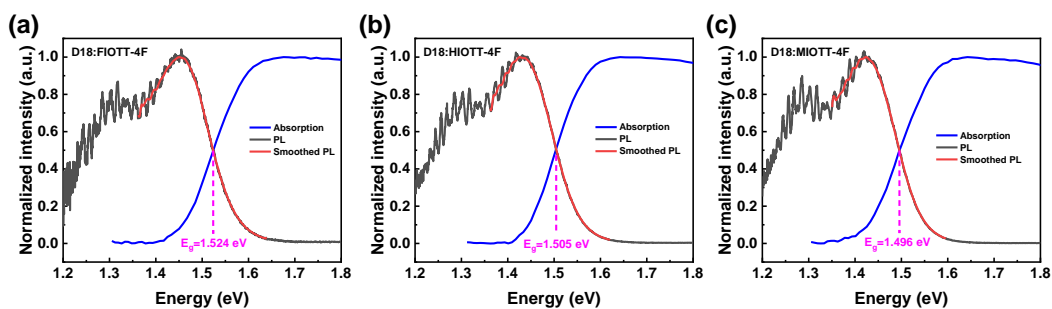


Fig. S25 E_g of different devices, calculated by absorption and PL spectra.

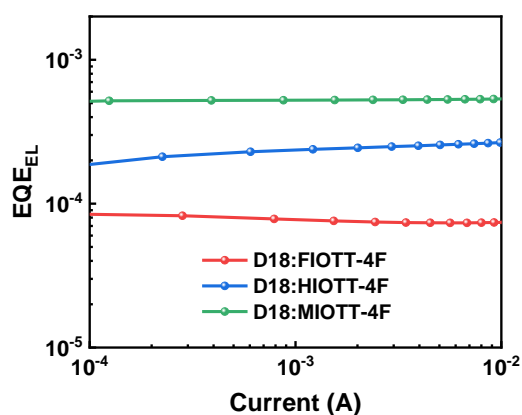


Fig. S26 EQE_{EL} characterization of different devices.

Table S2 Detailed energy losses of different devices.

Active layer	E_g (eV)	$V_{OC,SQ}$ (V)	ΔE_1 (eV)	$V_{OC,rad}$ (V)	ΔE_r (eV)	V_{OC} (V)	EQE_{EL}	ΔE_{nr} (eV)	ΔE_{loss} (eV)
D18:FIOTT-4F	1.524	1.254	0.270	1.167	0.087	0.923	7.75×10^{-5}	0.244	0.601
D18:HIOTT-4F	1.505	1.236	0.269	1.148	0.088	0.933	2.36×10^{-4}	0.215	0.572
D18:MIOTT-4F	1.496	1.228	0.268	1.151	0.077	0.956	5.24×10^{-4}	0.195	0.540

Notes: ΔE_1 comes from the radiative recombination from the absorption above the bandgap, calculated by SQ theory. ΔE_r comes from the radiative recombination from the absorption below the bandgap. ΔE_{nr} is nonradiative recombination loss, which can be calculated by the following equation:

$$\Delta E_{nr} = -kT \ln(EQE_{EL})$$

where EQE_{EL} is electroluminescence (EL) quantum efficiency of OSCs, k is the Boltzmann constant, and T is the Kelvin temperature^{5,6}.

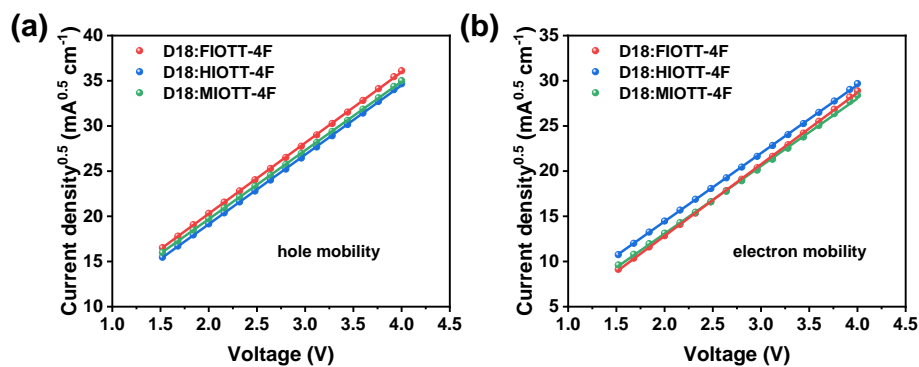


Fig. S27 $J^{0.5}$ - V curves of a) electron-only devices and b) hole-only devices.

Table S3 Hole and electron mobilities of different devices.

Active layer	$\mu_h \times 10^{-4}$ ($\text{cm}^2 \text{V}^{-1} \text{s}^{-1}$)	$\mu_e \times 10^{-4}$ ($\text{cm}^2 \text{V}^{-1} \text{s}^{-1}$)	μ_h/μ_e
D18:FIOTT-4F	2.17 ± 0.41	2.13 ± 0.45	1.02
D18:HIOTT-4F	1.88 ± 0.29	1.98 ± 0.37	0.95
D18:MIOTT-4F	1.92 ± 0.37	1.81 ± 0.19	1.06

Table S4 Summary of prefactors and lifetimes from biexponential fitting of the PB signals.

Active layer	A_1	τ_1 (ps)	A_2	τ_2 (ps)
D18:FIOTT-4F	0.673	0.20 ± 0.01	0.327	5.49 ± 0.49
D18:HIOTT-4F	0.791	0.22 ± 0.01	0.209	6.92 ± 1.12
D18:MIOTT-4F	0.744	0.38 ± 0.02	0.256	7.10 ± 1.50

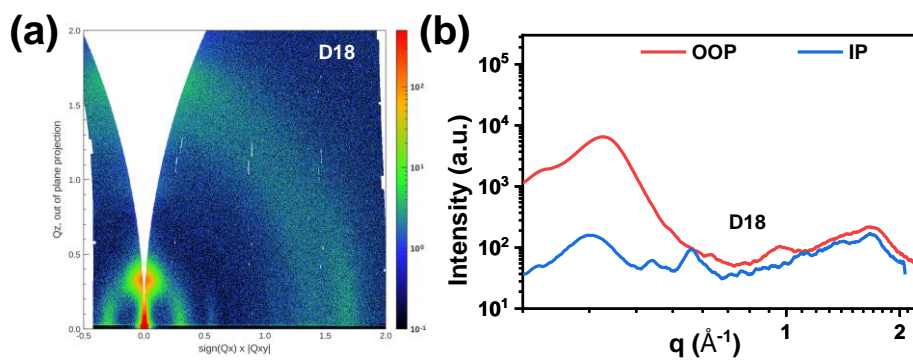


Fig. S28 a) 2D GIWAXS images and b) 1D intensity profiles of D18 film in out-of-plane (OOP) and in-plane (IP) directions.

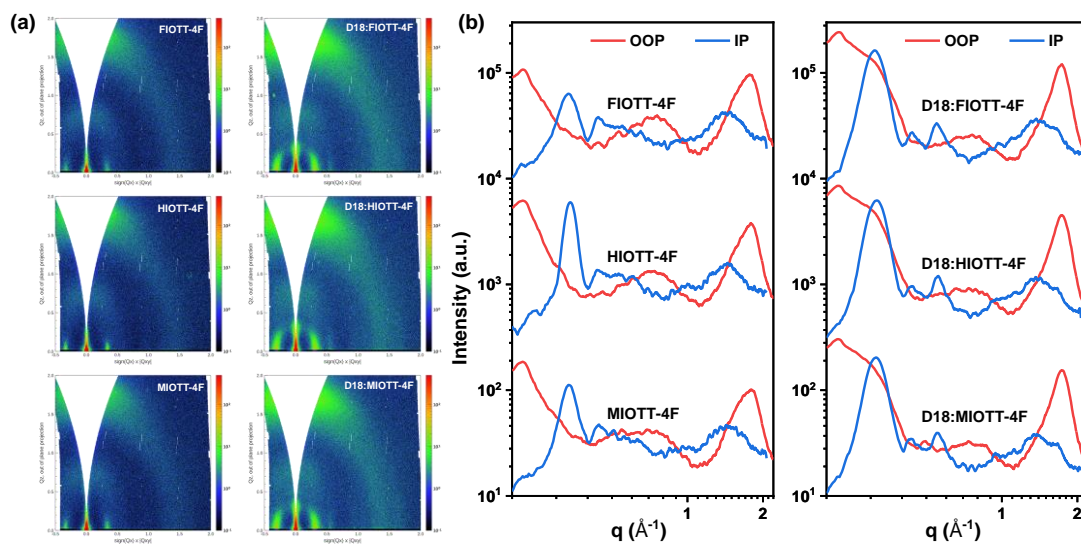


Fig. 29 a) 2D GIWAXS images and b) 1D intensity profiles of FIOTT-4F, HIOTT-4F, and MIOTT-4F pure films and D18:FIOTT-4F, D18:HIOTT-4F, and D18:MIOTT-4F blend films.

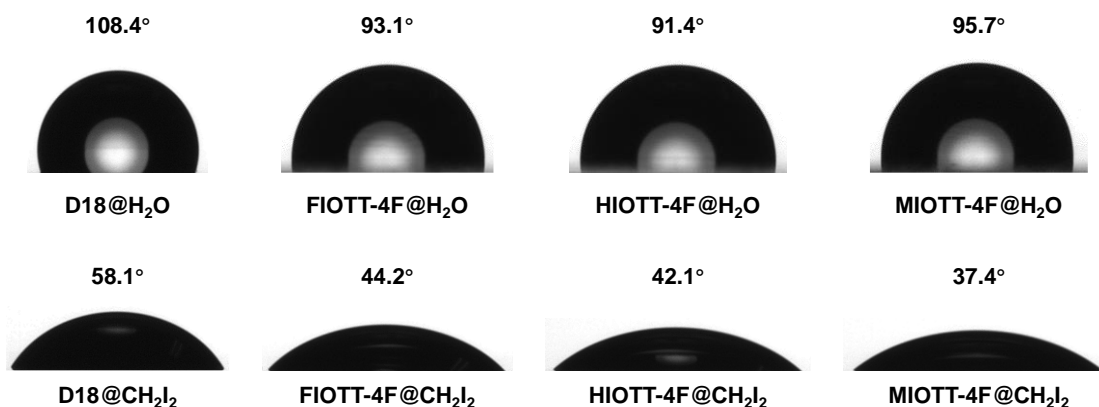


Fig. S30 Contact angle images of various films with water and diiodomethane (DIM).

Table S5 The contact angle of different films with water and diiodomethane (DIM), and the calculated surface energy.

Surface	θ_{Water} (°)	θ_{DIM} (°)	γ^p ^a (mN m ⁻¹)	γ^d ^b (mN m ⁻¹)	γ ^c (mN m ⁻¹)	χ^{D-A} ^d
D18	108.4	58.1	0.03	31.52	31.55	/
FIOTT-4F	93.1	44.2	0.72	36.93	37.65	0.27 K
HIOTT-4F	91.4	42.1	0.91	37.77	38.68	0.36 K
MIOTT-4F	95.7	37.4	0.13	41.80	41.93	0.74 K

^a Surface tension from polarity component. ^b Surface tension from dispersion component. ^c The total surface tension is calculated through the equation of $\gamma = \gamma^p + \gamma^d$.

^d The Flory-Huggins interaction parameter between the donor (D) and acceptor (A) is calculated with the equation of $\chi^{D-A} = K(\sqrt{\gamma_D} - \sqrt{\gamma_A})^2$.

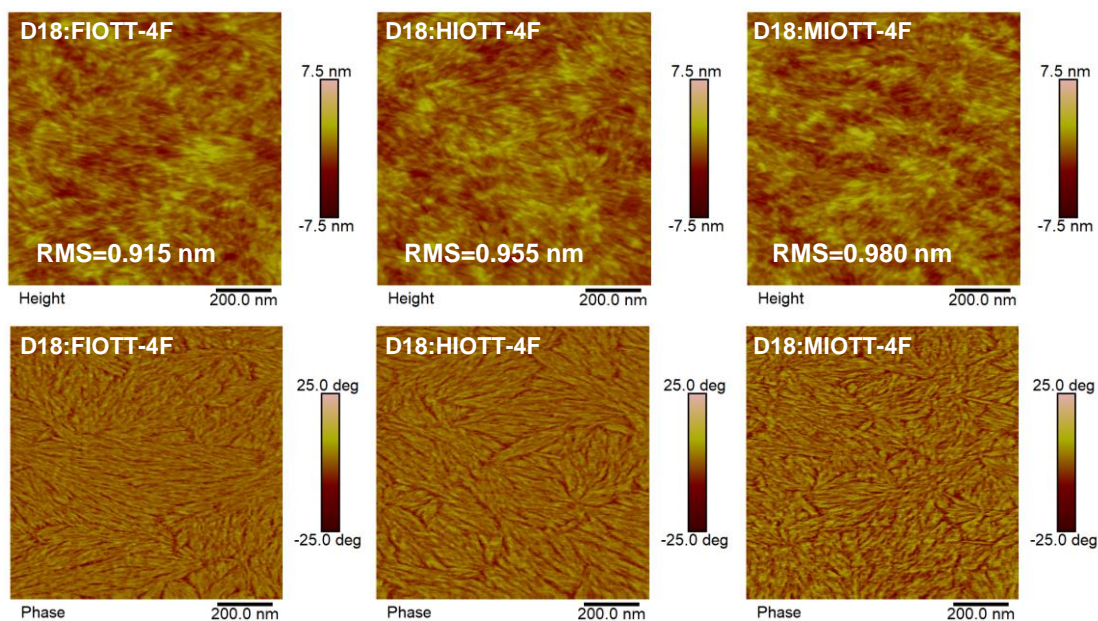


Fig. S31 AFM height and phase images for different films.

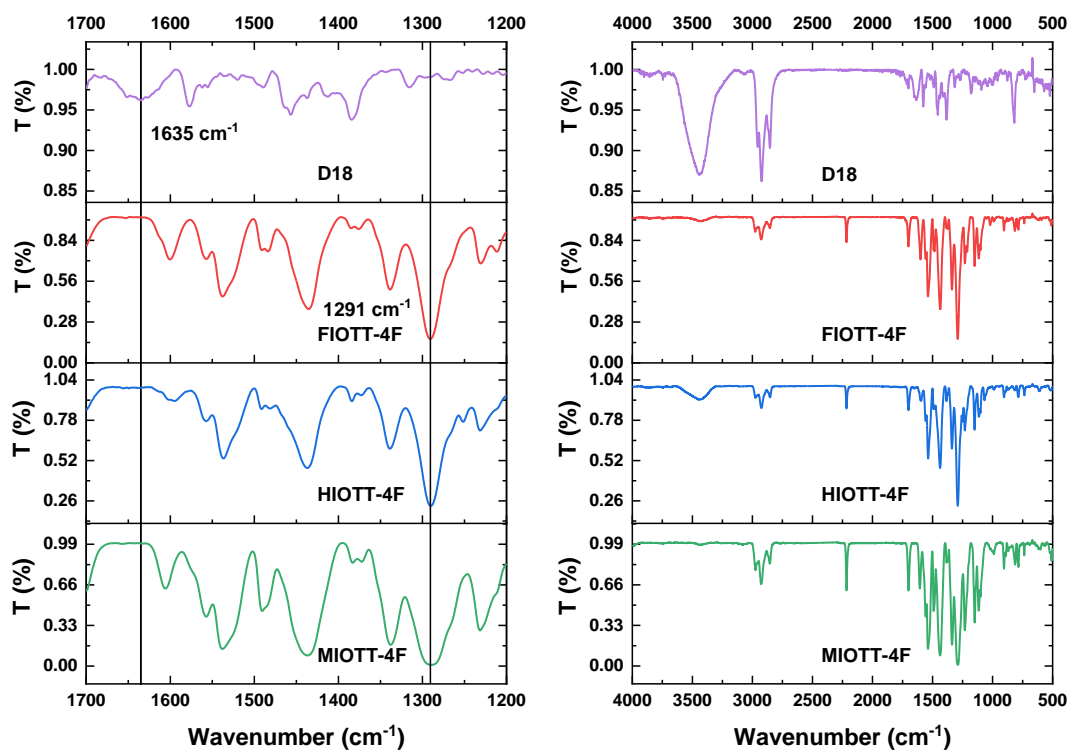


Fig. S32 FT-IR spectra of D18, FIOTT-4F, HIOTT-4F, and MIOTT-4F.

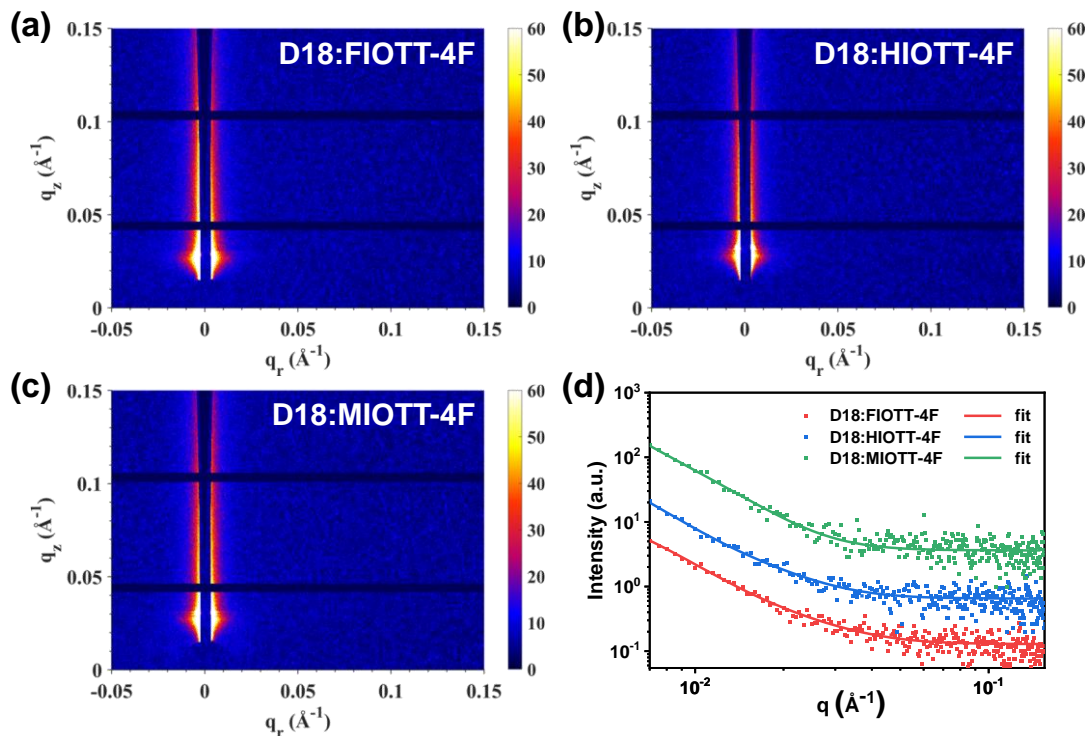


Fig. S33 a-c) 2D GISAXS images and d) 1D in-plane intensity profiles and fitting curves of D18:FIOTT-4F, D18:HIOTT-4F and D18:MIOTT-4F blend films.

Table S6 Fitted data of various films obtained from GISAXS measurement.

Blend	$2R_g^a$ (nm)	X_{dab}^b (nm)
D18:FIOTT-4F	17.4	17.7
D18:HIOTT-4F	23.8	24.2
D18:MIOTT-4F	42.6	31.9

^a The sizes of pure acceptor domain. ^b The sizes of amorphous intermixed domain.

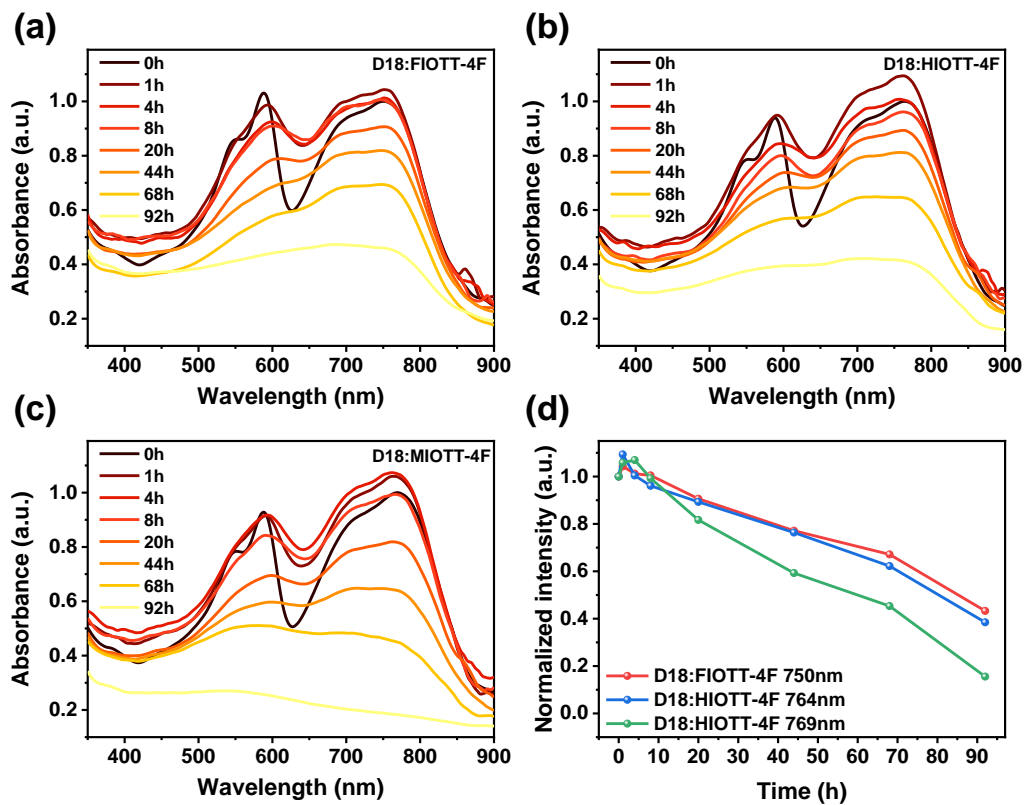


Fig. S34 The absorption spectra variation of a-c) blend films during the illuminating process. d) The change of absorption intensity versus photoaging time.

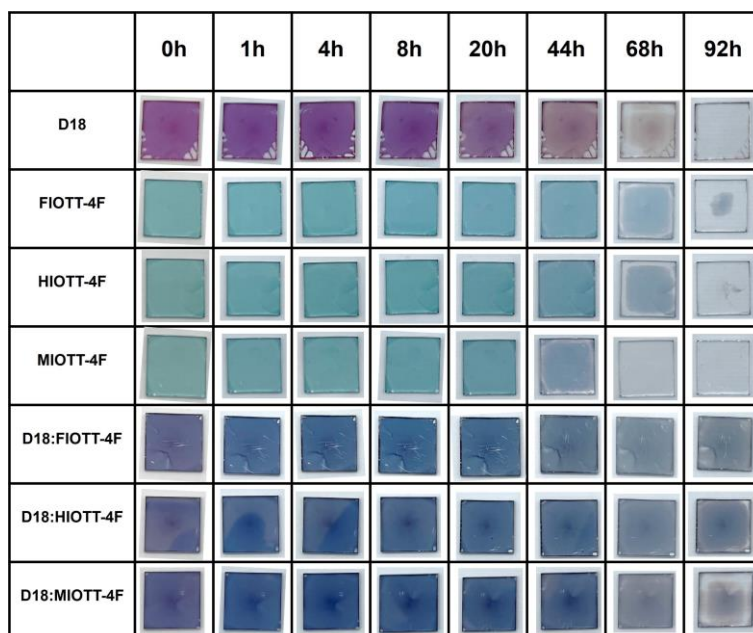


Fig. S35 Digital photos of different films in the photodegradation process.

Reference

- 1 Y. Shen, A. R. Hosseini, M. H. Wong and G. G. Malliaras, *ChemPhysChem*, 2004, **5**, 16-25.
- 2 L. Li, D. Qiu, J. Shi and Y. Li, *Org. Lett.*, 2016, **18**, 3726-3729.
- 3 P. A. Wender and D. Staveness, *Org. Lett.*, 2014, **16**, 5140-5143.
- 4 H. Fu, J. Yao, M. Zhang, L. Xue, Q. Zhou, S. Li, M. Lei, L. Meng, Z. G. Zhang and Y. Li, *Nat. Commun.*, 2022, **13**, 3687.
- 5 J. Yao, T. Kirchartz, M. S. Vezie, M. A. Faist, W. Gong, Z. He, H. Wu, J. Troughton, T. Watson, D. Bryant and J. Nelson, *Phys. Rev. Appl.*, 2015, **4**, 014020.
- 6 J. Liu, S. Chen, D. Qian, B. Gautam, G. Yang, J. Zhao, J. Bergqvist, F. Zhang, W. Ma, H. Ade, O. Inganäs, K. Gundogdu, F. Gao and H. Yan, *Nat. Energy*, 2016, **1**, 16089.